CT5318

Preliminary research for a marina in Byala

БЯЛА

winter 2006/2007

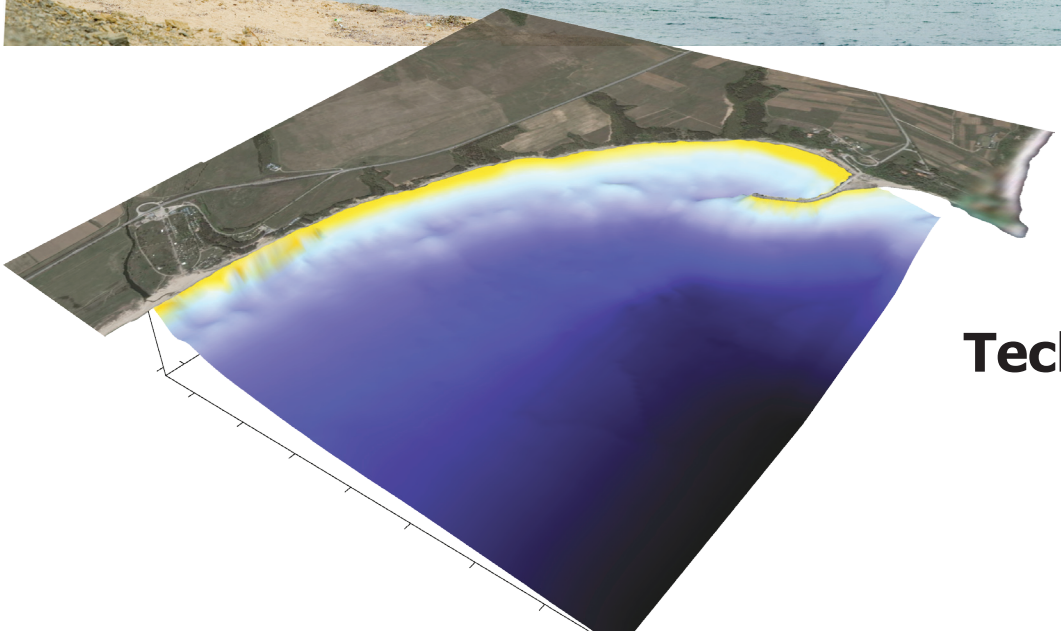

Technical report

Delft University of Technology

Preface

This is the final report of the project 'Fieldwork Coastal Engineering', part of the Master studies Hydraulic Engineering of Delft University of Technology (TU Delft). It has been made by students of the TU Delft, in cooperation with students from the University of Architecture in Sophia. The fieldwork took place in Byala, Bulgaria, between 5th October and 12th October 2006.

The aim of the fieldwork is to give the students insight in how to set up a measuring campaign, how such a campaign will be executed and how it should be reported. This year there is also a cooperation with a coastal development project, Marina Black Sea. The data, collected during the measurements, have been used to make a preliminary design for a breakwater that can protect the future marina, which is being developed at the moment.

This report is above all a technical report. The data collected with the measurements is presented, as well as the methods used for the measurements. Furthermore, the preliminary design of the normative cross-section of the breakwater has been included. The report can be used as a starting point by those who will make the final design for the breakwater.

The students are grateful to Mr. Verhagen and Prof. Daskalov, the teachers from Delft and Sophia, for their support during the fieldwork. We also would like to thank Mr. Savov sr. and Mr. Savov jr. for their efforts in helping us with practical matters when they could. Furthermore our thanks go to Mr. Nollen from Marina Black Sea for giving us the chance to go to Byala for this fieldwork. Last but not least we would like the Bulgarian students for their help during the measurement campaign and for the great time we spent together!

Delft, December 2006

Paula van Baaren
Priscilla Bonte
Matthijs Boon
Maria Bougdanou
Lennart Burg
Haiyang Cui
Thijs Damsma
Erik van Eekelen
Pieter van Geer
Dehua Gu
Jirat Laksalanamai
Claire van Oeveren
Jorg Oosthoek
Arend Pool
Jules Schmedding
Noud Schoenmakers
Paul van Steeg
Pétur Sveinbjörnsson

Table of contents

1 Introduction

On the 1st of January, 2007, Bulgaria will be part of the European Union. This is expected to increase tourism along the Bulgarian Black Sea coast further. In this light, the development of a marina has started between the towns of Obzor and Byala.

This marina needs to be protected by a breakwater to ensure a calm and comfortable water surface within the marina area. For the determination of the local boundary conditions and a preliminary design, a group of students from Delft University of Technology (Faculty of Civil Engineering) and University of Architecture (Department of Hydraulics) from Sophia has been invited. For the students from Delft this project is also part of their studies (for the subject Fieldwork Coastal Engineering).

The aim of this report is to present the results of the measurements undertaken during the fieldwork in Bulgaria and the preliminary design of the cross-section of the breakwater needed to protect the marina during design conditions. This preliminary design is based on the preliminary boundary condition of a design wave height.

The measurements that have been undertaken during the campaign are various. At the Byala fishermen's harbour, the state of the existing breakwater has been observed and the dimensions of the Tetrapod armour layer have been measured. The bathymetry of the project area has been measured and the morphological situation has been observed. Furthermore the beach and revetment profiles in the project area have been measured. Visual wave observations and pressure meter measurements have been done at two different locations: Byala and St. Constantine. Finally, in a regional quarry the dimensions and quality of rock have been measured to determine if the rock is suitable for the designed breakwater.

The structure of this report is as follows. In chapter 2 several beach cross profiles are presented, as well as a description of the local geological situation. This data, together with depth measurements, are the input for a bathymetrical map, which can be found in chapter 3. The bathymetry influences the morphology of the area through wave action. The morphology is treated in chapter 4. In chapter 5 the local soil properties can be found, expressed in sieve curves. Chapter 6 consists of the visual wave observations and data from a pressure meter. Both techniques lead to values for a significant wave height. In chapter 8 the results of the observations and measurements on the breakwater are presented. From the measurements on the Tetrapods, a design wave height has been calculated. The preliminary design for the marina breakwater is presented in chapter 9. Finally, in chapter 8 the results of a quarry visit are found. In this quarry rock measurements have been done to determine if the rock is suitable for use in the designed breakwater.

2 Beach profiles

The aim of measuring the beaches is to draw the alignments of the beaches and locate the position of the beaches. Analyzing these results can tell something about the dynamic behaviour of these beaches and the response on severe wave attack.

To determine the alignments two different methods were used. The first method was applied on the beach located north from of the revetment. A scale was used to measure the elevation, using the horizon as a reference level. The coordinates where determined by measuring the distance from a fixed point. The second method, applied on the southern beach, used a levelling instrument and a scale to measure the elevation. The coordinates of the measurements were obtained by using a GPS. In the following chapters about the measurement approach a more detailed description is given.

After the coordinates of the measurement points were collected, a figure of the beach profile can be drawn. A plot of the different cross profiles from the beaches has been made by using Excel. A general overview of the beach elevation has also been made with use of the program Surfer. By combining the coordinates and the elevation of all cross profiles a contour map of the beaches has been drawn.

A further analysis of the beach was made by taking sand samples from different parts of the beach. Sieving these samples will tell something about grain size distribution along the beach (chapter 5). These results are important to analyze the morphologic behaviour of this area. In this part of the report the position where these samples were taken is presented. The resulting conclusion with respect to morphology is written down in the accompanying part of this report. The description and characteristics of the beach are helpful to give some advice about developing the marina and villa's for this project.

2.1 Measurements of the northern beach

General description of the northern beach

The most remarkable features of the beach north from the revetment are the steep cliffs at the end of the beach. These cliffs consist of hard layers of compressed clay. At the foot of these cliffs there is a sandy beach which is approximately 8 to 15 meters wide. The more northern parts of the beach become smaller where there are only a few meters of sands before the waterline. The clay layers, which the cliffs also consists of, are coming up a few meters behind the waterline in the sea. Figure 2.1 gives an indication of the appearance of the beach. Figure 2.2 shows the rising clay layer in the water

figure 2.1 Overview of northern beach

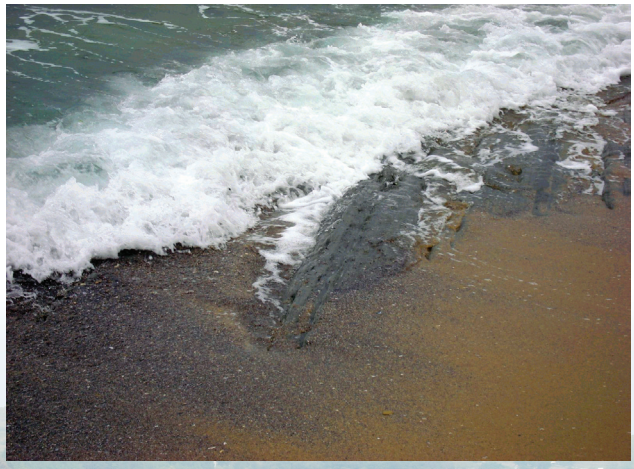

figure 2.2 Clay layers at the waterline

Method

To determine the coordinates of the measurement point a reference point was needed. Since the baseline was not ready at the beginning of the measurements, the mean waterline was used as a longitudinal reference. Perpendicular to the waterline, cross sections of the beach were measured. The distance from the reference point (end of the revetment) was measured with a measuring tape. According to these measurements it was possible to recalculate the coordinates.

When a point was selected along the waterline the scale was put at the distinguished point between clay and sand in the water. At the foot of the cliff the value was determined by observing the level of the horizon with respect to the scale. By using a stick with a fixed length the eye of the observer is on the same level every measurement. After recording the elevation of the first point the scale was moved towards the observer and the difference in distance was measured. Several measurements were taken and by using the difference between the values and the distance between the measuring points, a cross profile was determined. Figure 2.4 gives an illustration of the applied method and figure 2.3 shows a measurement.

figure 2.3 Measuring method

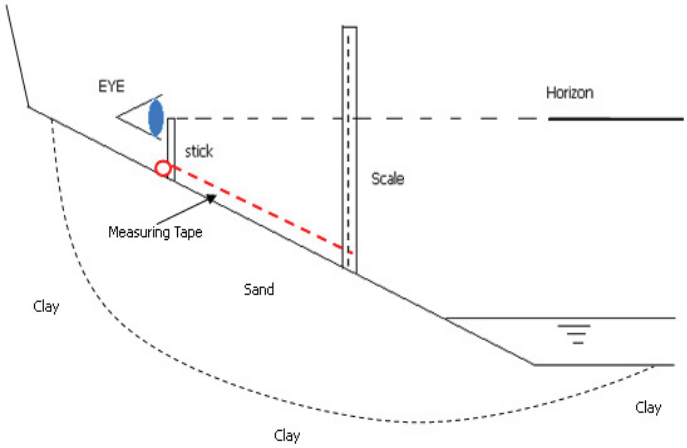

figure 2.4 Measuring the elevation

Analysis of the cliff

The cliff on the northern side of the beach consists of hard dry clay. The structure of this soil is layered (figure 2.5). It is clearly visible that there are layers present which consist of more sandy clay types. It should be noted that along these layers it is possible that al slip circle forms. Figure 2.7 shows the principle schematically. During the observation, small landslides were observed. Because landslides occur along large parts of the Bulgarian coast it is important to keep this in mind (figure 2.6). During a storm the force of a wave will increase. When the toe of the cliffs is exposed to this wave load, it could lead to erosion at toe. Thus leading to steeper cliffs and increasing the possibility of a landslide.

figure 2.5 Layered structure of the clay

figure 2.6 Small landslide

figure 2.7 Slip circle of the cliffs

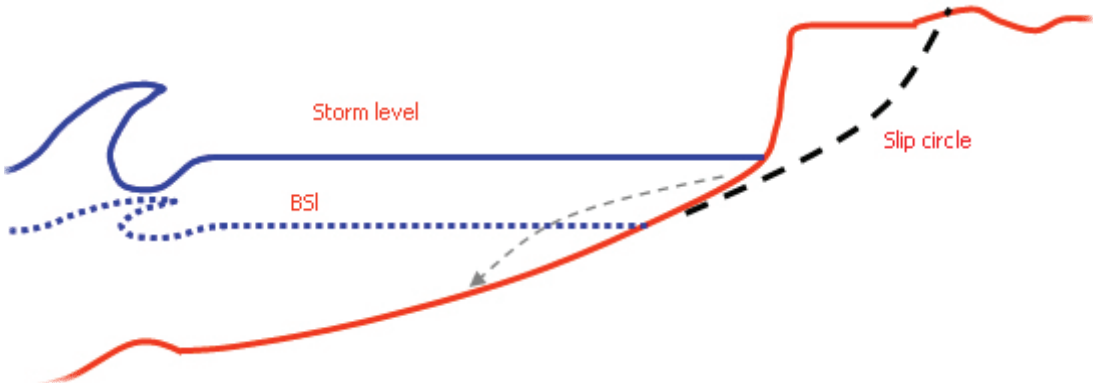

The withdrawal of land is very slow; in the long run this gradual process might lead to more erosion. At the moment, tree roots retain the soil. Further stability of the cliffs can be gained by a drainage system. It was observed, that this system is used at various places.

2.2 Measurements of the southern beach

figure 2.8 Overview of southern beach

General description of the southern beach

The southern beach is considerably different than from the northern beach. South of the revetment there is are no cliffs close to the beach. This results in a beach that is wider; approximately 40 meters (figure 2.8). The clay layer that appears a few meters in the water is not present at this beach either. The soil around this beach consists mainly of sands till a certain depth.

Method

The southern beach was measured in a slightly different way. In stead of the "eye-horizon" method a levelling instrument was used. In this situation the levelling instrument was placed perfectly horizontal on a baseline and levels where measured from scale. By replacing the scale more forward other points could be measured.

For the location of the measurement points a GPS was used. For every point the coordinates were recorded. In this way a coordinate was coupled to a certain elevation of the beach.

figure 2.9 Measuring the beach by using a leveling instrument

2.4 Contour map

With help of the program SURFER a contour map is drawn of the two beaches. A general view of the contours of the beaches is obtained. A more accurate presentation of the beach levels is presented in the appendix with the cross profiles plotted in Excel. In figures 2.10 and 2.11 show the elevation of the beaches at the north and south side of the revetment. It is important to notice that surfer interpolates and extrapolates between different points. This map does not give an exact plot of the beach but gives a more general overview. The zero line gives the position of the waterline. The cross points are the positions of the measured points.

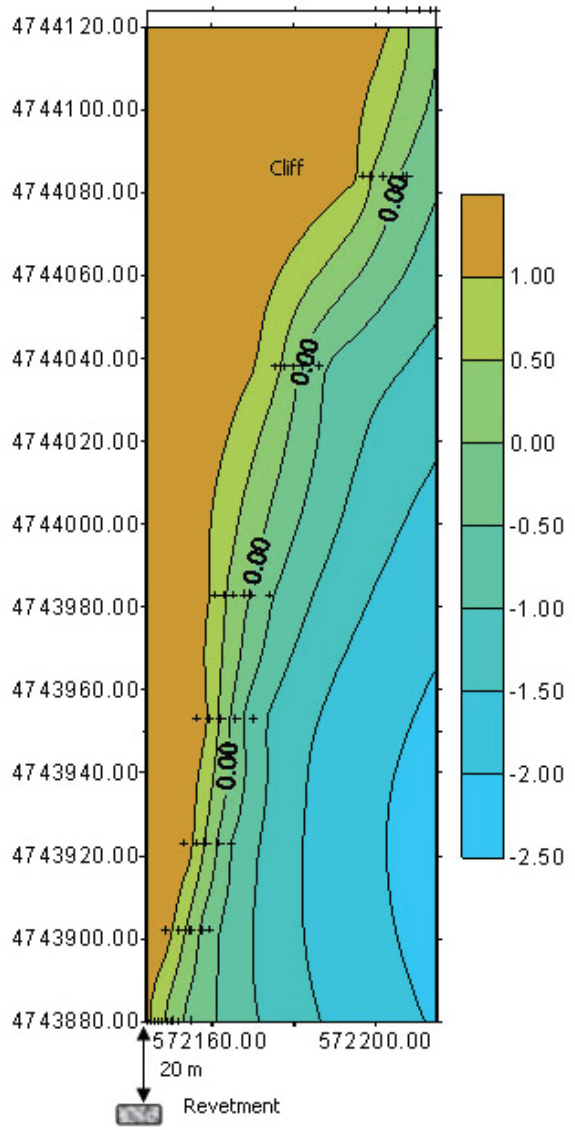

figure 2.10 Northern beach

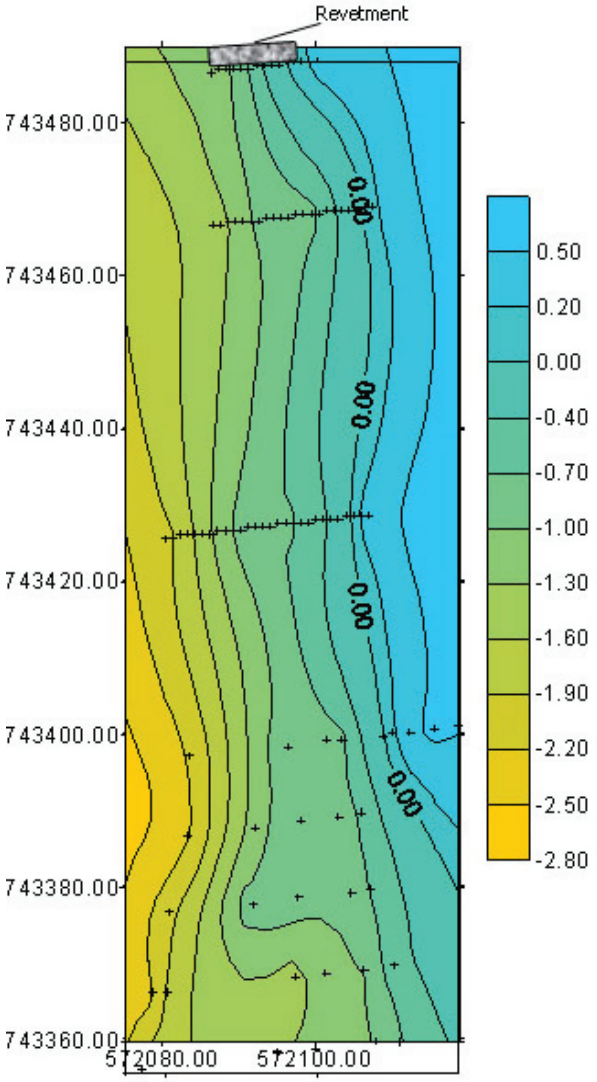

figure 2.11 Southern beach

2.5 Conclusion

The measurements of the northern beach profile clearly mark the wave attack from the last storm. The sharp drop in elevation indicates the maximum run-up. If a more severe storm occurs the profile will be redistributed and the shape of the beach changes.

Landslides from the cliffs can give the beach a different appearance as well. It is therefore important to notice that the measured cross profiles are snapshots in time.

The southern beach does not show the sharp drop in the cross profile. The gradient of the beach is less steep compared to the northern beach. It can be seen from the plotted profiles the gradient is much steeper near the waterline. This is caused by the redistribution of sand by wave run-up. Dynamical changes of the southern beach will be smaller than those of the northern beach. The wider southern beach with a flatter slope will give fewer changes in the amount of elevation differences.

Finally a remark about the cliffs should be made. Special attention should be given to the planning of the location of vacation residences. The erosion of these cliffs forms a danger for houses standing close to the edge. Wave attack might lead to more steepness. Tree roots act as soil retainer which leads to stability. Chopping down of trees might lead to additional erosion. A drainage system will increase stability. Housing on top of the cliffs should be protected against erosion.

3 Bathymetrical map

3.1 Method & Equipment

To map a coast, equipment is needed for measuring purposes. A boat, with a GPS and a echo sounder is needed off-shore. In chapter 3 the beach profile measurements were discussed. The resulting data is included in the eventual depth chart. This will lead to data points; in this case south of the Byala breakwater. The data needs to be interpreted and therefore a reference is needed. This will be discussed below.

GPS

Two standard handheld Garmin GPS receivers were used. The accuracy was 5 meters at best in the horizontal plane, but strongly dependent on satellite coverage. GPS accuracy near the steep cliffs was predominantly worse than 20m. The accuracy of altitude measurements done with the GPS were in the same range.

Echo sounder

An echo sounder/fish finder was used for depth measurements. This echo sounder has an accuracy of 0,10 *m*. Other factors that influenced the accuracy of the measurements are

- *The angle of the echo sounder:* The echo sounder must be mounted in a way that it measures in a vertical line. Due to pitching and rolling of the boat and the primitive mounting of the fish finder this ideal situation is approached to a certain degree. At the time the measurements were taken the wave height from visual observation was +/- 30 *cm*.
- *The calibration*: The rope that is used to calibrate the fish finder must also go straight downward, which means that the boat must stay in exactly the same position during the calibration.

Taking into account the above the accuracy of the depth measurements is estimated to be 0,30 *m*.

Area of interest

The area of interest in longshore direction is from the existing breakwater southward to a revetment, a stretch of some 1600 meters. Measurements were made up to 500 *m* from the coast.

Reference height

Depth measurements are related to the water level. To relate this to the heights on the map two measurements were taken from the quay wall for which the height was indicated on the map relative to chart datum (according to mr. Daskalov MSL = CD + 0,20 *m*). This was done using a theodolite and a vertical ruler. Using the difference between the water level and a fixed point on the breakwater and the difference between this point and CD as indicated on the map the present water level can be related to CD. Because of wave action the accuracy in determining the water level was no more than 5 *cm*. The two measured water levels related to CD differed 10 *cm*. This might imply that the breakwater has subsided.

figure 3.1 Reference height

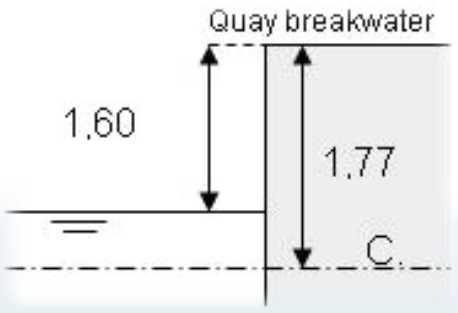

From these measurements the still water level was calculated at CD + 0,17 meters. Because of inaccuracies in these measurements and possible water level variations in time, the accuracy of this measurement is estimated to be +/- 15 *cm*.

Reference location

On the map (see appendix III) a 100 *m* grid is plotted, oriented north. However the relative position of this local grid to the Universal Transverse Mercator (UTM) system was unknown. To relate the GPS coordinates in UTM to this grid on the map a accessible and recognizable calibration point was needed.

3.2 Data processing

Data acquired by the different measurement methods are processed using Microsoft Excel. Both data from the echo soundings and beach profile measurements are related to chart datum (which is 17 *cm* lower than the water level at that moment). All GPS measurements representing the waterline are manually set to have a zero meter height. In addition to that also a number of data points representing the breakwater in the old port have been taken from the map. These different data sets are combined and exported for use in the SURFER program.

figure 3.2 Pattern sailed

The data is imported into SURFER using the kriging gridding method with an anisotrophy ratio of 1 and an angle of 0 degrees. SURFER gives the opportunity to plot all measurement points. The result is shown in figure 3.2. Measured data are denoted by a small triangle. Data created to fill the areas in which no measurements are done including the breakwater at the harbor are denoted by the crosses.

The kriging method was used because it is known to give the best results. However it is still possible that numerical artifacts occur. The most obvious ones were corrected using additional data points. Also interpolation is difficult over discontinuities of the bottom profile (vertical jumps), this is the case at the quay wall on the inside of the breakwater.

The resulting bathymetrical map is included in figure 3.3, measurement data and results as well as the used artificial points at the boundaries can be found in appendix III and IV.

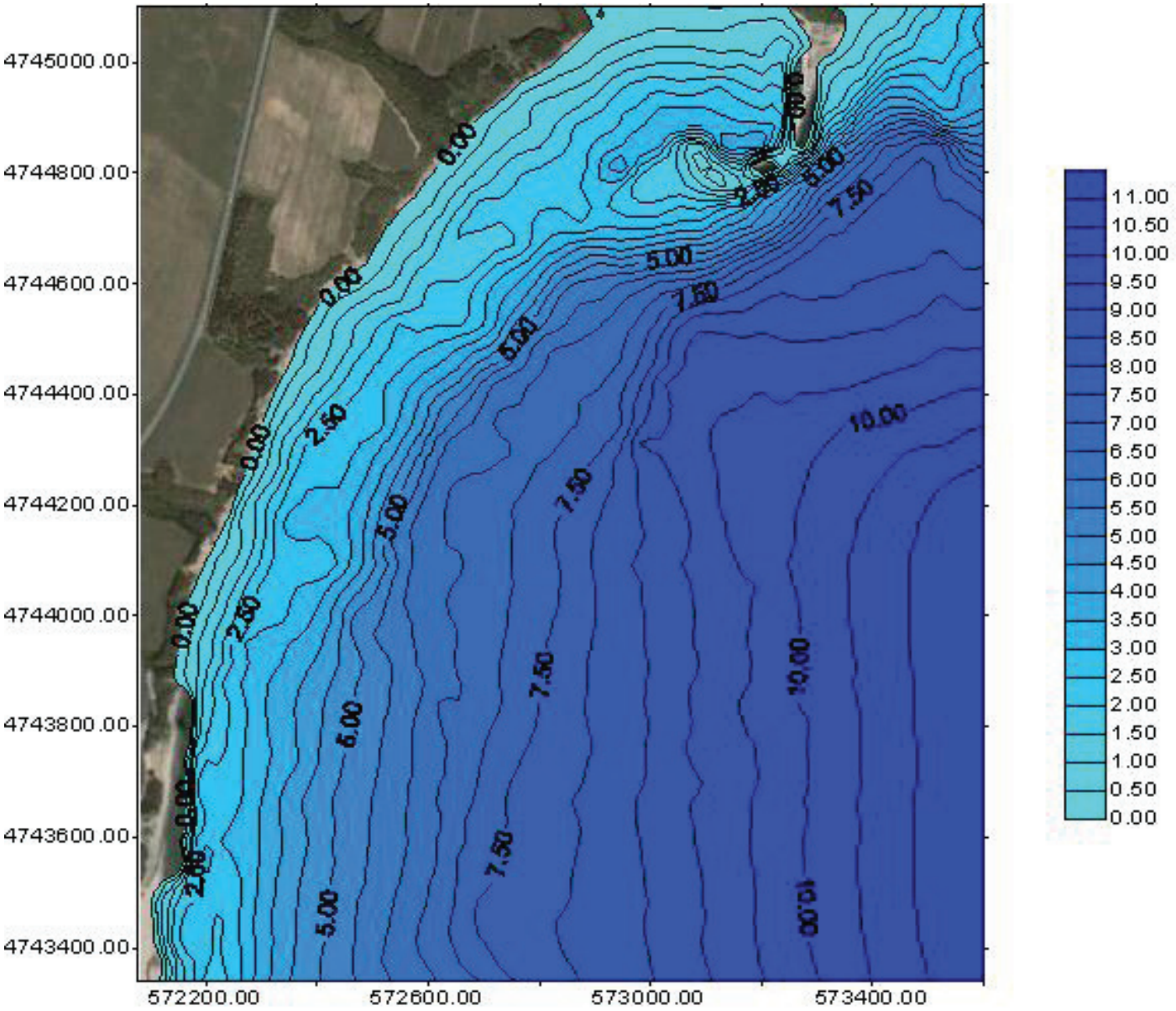

figure 3.3 Bathymetrical map

4 Morphology

4.1 Introduction

For the construction of a marina near Byala it is of great importance to get more insight into the morphological processes along that part of the coast. At the moment of writing a fishing harbour is present, approximately 1 *km* north of the project location of the new marina. For the construction of the fishing harbour little was know regarding the morphological processes. Therefore the fishing harbour encounters problems with respect to sedimentation; the entrance channel becomes too shallow. A better insight in the morphological processes could have prevented these problems.

To prevent sedimentation problems in the new marina the morphological processes in the area of interest need to be investigated. These investigations consist of two parts. The first part consists of visual observations, the large scale processes can best be observed on a satellite photograph and the smaller scale processes have been studied in the field. For the second part of the investigation sand samples have been taken at different locations along the coast. These samples have been discussed in chapter 2.

The satellite photograph in figure 4.1 shows the above described area of interest. The red circle indicates the planned location for the marina. At the moment of writing a revetment and a small quay wall are present at the project location. For further description of the coast the area is divided into two sections: section A is situated south of the project location and section B is located at the north of the new marina.

figure 4.1 Overview of coast near Byala, red circle indicates the planned project location

The dominant wind direction at the coast of Bulgaria is North-East, with strong north-eastern storms in wintertime. These storms are responsible for the largest contribution of the sediment transport along the Bulgarian coast. This transport is directed from North to South. Furthermore a different type of wind occurs in summertime. The temperature difference between land and sea causes a landward directed sea breeze. This sea breeze generates sand transport in northern direction. The sea breeze is much weaker than the winter storms and therefore is able to transport a smaller amount of sand. However, the combination of these two sediment transport processes can lead to problems a harbour.

The sedimentation of the entrance channel of the fishing harbour can be explained by these two described sediment transport processes. The breakwater prevents the winter storm driven sediment from entering the harbour. However, the sea breeze driven sediment transport is directed from south to north and is able to enter the harbour. Because the harbour is sheltered from the winter storm the sediment settles inside the harbour and is not brought into the system again by the winter storm. The result is a net sediment transport into the fishing harbour.

4.2 Visual observations from satellite

On the right-hand side of the satellite picture an outcrop can be observed. This outcrop probably consists of hard material, this is concluded based on how it protrudes into the sea. If it would consist of soft material it would have eroded, leaving a straight coast line. The breakwater of the existing fishing harbour is situated south of this outcrop. South of this fishing harbour the coastline consists of a sandy beach, this part of the coast is divided into two sections with different properties. The satellite picture directly shows that the beach at section A is much wider than the beach at section B. The narrow beach at section B indicates an eroding coast. Another typical feature is the shallow area in the sea, stretching from the tip of the breakwater to the coastline near the revetment. It seems that sediment is transported along this bar. This assumption is supported by the small width of the beach in section B, the sand probably passes this part of the coast and only comes to shore at section A.

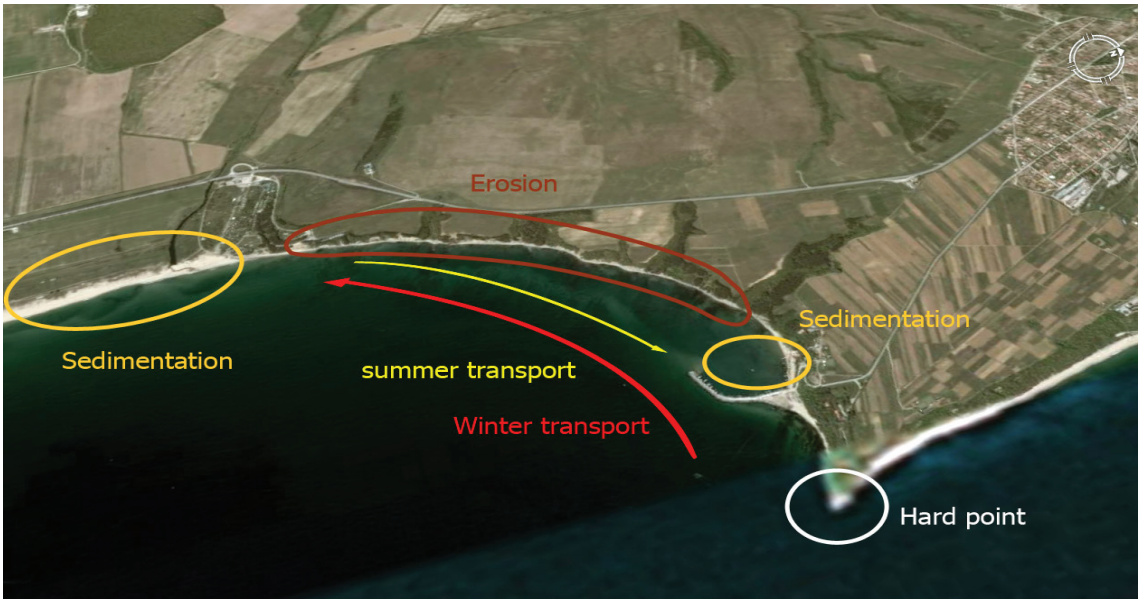

figure 4.2 Overview of morphological processes along the coast near Byala

The above figure shows a global overview of the morphological processes which have been identified up to this point.

4.3 Visual observations in the field

The area in section B is difficult to characterise based on the satellite picture only, therefore visual observations where done in the field. A division of the observations is made for four areas along the coast:

- Outcrop;
- Fishing harbour;
- Coast at section B, between fishing harbour and project location;
- Coast at section A, south of the project location;

Outcrop

The outcrop has been studied up-close. The outcrop is very steep and consists of very hard material. The material has been identified as cemented sand or sandstone. Just south of the outcrop the shore consists of a narrow beach. On this beach boulders of the same material can be found. This indicates that during heavy storms material is broken of the outcrop, which gradually erodes and causes sediment transport south of the outcrop. The boulders on the beach do not have sharp edges, but have a smooth shape. This supports the assumption that the boulders gradually erode. The pictures on the next page show the texture of the outcrop (figure 4.3) and the smoothened boulders on the beach (figure 4.4).

figure 4.3 Texture of the outcrop

figure 4.4 Smoothened boulders near outcrop

Fishing harbour

Problems regarding sedimentation in the fishing harbour have already been described in the introduction. Observations indeed show a shoal at in tip of the breakwater. This can also be observed in the satellite photograph. This shoal is probably caused by settlement of the long-shore transported sediment behind the tip of the breakwater. The area behind the breakwater is sheltered, therefore the flow velocity and the wave action are reduced hence sediment will settle. This sediment of the shoal is moved into the harbour by the sea breeze in the summer.

The beach inside the harbour, used for the maintenance of boats, is relatively wide compared to the beach south of the harbour. Probably this is also caused by the summer sediment transport. The sediment is then transported into the harbour and will not be transported back in winter due to sheltering against north-eastern wind.

Coast at section B, between fishing harbour and project location

The general characteristics of the coast at section B are steep high cliffs with a relatively small sandy beach in front of those cliffs. The cliffs are approximately 10 to 15 meter high and consist of clayey material. This material is very brittle and can easily be broken by hand. It is clear that these cliffs are subject to severe erosion because of the roots of trees hanging out of the cliff. This is illustrated in figure 4.5.

Furthermore traces of landslides can be observed in the field. Another phenomenon discovered during the fieldwork is the compositions of the cliff. The cliff consists of several layers as can be seen in figure 4.6. Originally the layers were horizontal due to deposition of sediment. Due to landslides the layers have become almost vertical.

This erosion is caused mainly by wave attack at the toe of the cliff, which makes the slope unstable. Because the cliff is very steep, heavy rainfall can easily erode part of the cliff.

figure 4.5 Roots of trees showing

figure 4.6 Different clay layers

Figure 4.5 also shows that the beach in front of the cliff is very narrow. Measurements showed a width varying from approximately zero to seven meters. The sand layer on the beach is very thin and decreases even further near the outcrop, where it eventually disappears. Particularly in the water large parts of the clay layer are exposed. The assumption is made earlier that the cliff protruded much further into sea and due to erosion the cliff has retreated. The large clayey parts in the water support this assumption. Sand eroded from the outcrop and sand originating from further north and from the south is transported to this part of the coast and deposited in small amounts. The slope of the beach is very mild as is also the slope further seaward. The sea remains therefore very shallow until relatively far offshore

Coast at section A, south of the project location

The coast at section A consists of a well developed sandy beach; no cliffs are present close to the shoreline. The beach has a width of approximately 10m and an impression of this beach can be seen in figure 4.7. Due to the sandy beaches this location is attractive for project developers to build holiday resorts.

Based on the consideration earlier in this chapter this beach is formed because the sediment transport, originating from the outcrop and farther north, attaches to the shoreline at this location. Wave action moves the sediment towards the coast. The slope of the beach is very mild, as is to be expected in case of a sandy coast.

figure 4.7 The beach south of the revetment

4.4 Sand samples

Based on the results of the sieving analysis (see chapter 5) an attempt is made to find similarities or differences in the sand properties at different locations. However, the D_{50} and the ratio D_{60}/D_{10} of the samples do not show similarities or differences which can be used to analyse the morphological processes. This may be caused by a number of reasons. First of all the samples were most likely taken at different distances from the shoreline. In the field has been observed that the sand far from the coastline (land inward) is finer than the sand near the coastline. Second of all, the samples were probably taken in different ways. For instance, some samples contain only sand of the top layer with another sample may be taken somewhat deeper. Differences have been discovered. Samples taken very near each other show different results in the sieving analysis.

4.5 Relevance for construction of the new marina

The processes described in the previous paragraphs will have effects on the future marina. The marina will be constructed at the interface of two very different stretches of the coast (figure 4.1). Section B consists of a severely eroding, clayey coast, characterised by landslides. On the other hand, the coast at section A consists of a relatively wide sandy beach, with a shallow foreshore as a result. This shallow foreshore has two effects. On one hand it causes the higher waves to break at deep water, so energy has been dissipated before the waves reach the marina, on the other hand the depth of the harbour needs to be sufficient for boats to be able to sail.

Because the higher waves break before reaching the marina the height of the breakwater sheltering the marina can be relatively small and therefore the costs of the breakwater can be reduced. The shallow foreshore may cause problems regarding the draught of ships. This is the case for both the marina itself and the entrance channel. If the water depth near-shore is too shallow two measures can be taken. The marina can be extended into the sea or dredging works need to be performed to increase the water depth locally. However, the design ship has not been determined yet at the moment of writing, therefore no conclusions can be drawn regarding the necessary water depth.

To prevent sedimentation of the marina in winter time it is important that the breakwater shelters the marina from the north-east side. Furthermore it is favourable if the entrance of the marina is situated on the landward side of the dominant sediment transport zone. This zone is located at a depth of approximately 4 *m*, the largest quantity of sediment is transported in this zone. Therefore it is important that the entrance of the marina is not situated in this region. When the entrance is situated in smaller water depth there will certainly be sediment transport at that depth. However, the waves will then be smaller and are therefore able to transport much smaller quantities of sediment. These relatively small amounts of sediment are not likely to cause serious sedimentation problems in the marina.

5 Sieve analysis

To be able to make predictions and computations about the morphological behaviour of the area of interest, the structure and composition of the sand from several beaches in the area have to be analysed and compared. Multiple sand-samples were taken from varying heights on the beach profiles. These samples were brought back to the university laboratory, in order to perform a sieve analysis. Of every sample the D_{50} was determined, as well as the ratio D_{60}/D_{10}.

The D_{50} is defined as the sieve diameter that is passed by 50 percent of the sand particles during the process of sieving. The D_{10} and D_{60} are similarly defined. These are all statistical values and the reliability of the outcome depends to a large extend on the quality of the sample and the sieving procedure. With the D_{50} the median grading of a sample is characterized, with the ratio D_{60}/D_{10} the width of grading is characterized.

5.1 Sieving method

The samples need to be completely dry before they can be sieved. Therefore each sample (with an average weight between 150 and 200 grams) is first left to dry on a heater for 10 minutes (figure 5.1). After heating, the sample is ready for sieving.

This sieving is done in a large stack of sieves (figure 5.2), with decreasing mesh size from the top down. For the purpose of this survey it is not necessary to know the exact grading of the sand, an approximate grading will suffice. Since all samples are within a certain range of grading, not all sieves have been used. The coarsest sieves on top (mesh size > 1400 μm) as well as the finest sieves on the bottom (mesh size < 125 μm) were left out. Therefore, the number of sieves in the stack was narrowed down to 13 sieves, with mesh sizes decreasing from 1400 μm to 125 μm.

figure 5.1 Drying the sand

figure 5.2 Stack of sieves

figure 5.3 Sieving machine

To begin the sieving, the dry sample is placed in the top sieve. The whole stack of sieves can then be placed on a machine (figure 5.3) that intensely vibrates the stack until all particles have fallen into the appropriate sieve. After 16 minutes of sieving the particles will no longer move downwards to finer sieves. This duration was therefore used.

5.2 Results

When the sieving is finished, each sieve is carefully emptied and its contents are weighed. In this way for each sieve diameter a corresponding fraction of the total mass is obtained. The results are put in an Excel sheet, for further computations. As an example, the results of one sample are show in the table 5.1.

table 5.1 Results sieve sampling

Sieve diameter (mm)	1,400	1,180	0,850	0,710	0,600	0,500	0,425
Weight (*g*)	2,325	2,104	12,804	13,678	24,941	32,321	24,824
cumulative (*g*)	2,325	4,429	17,233	30,911	55,852	88,173	112,997
cumulative (%)	1,473	2,807	10,921	19,590	35,396	55,879	71,611
% passing sieve	98,527	97,193	89,079	80,410	64,604	44,121	28,389
P (passing)	0,985	0,972	0,891	0,804	0,646	0,441	0,284
Gauss value	2,177	1,910	1,231	0,856	0,375	-0,148	-0,571

Sieve diameter (mm)	0,355	0,250	0,212	0,180	0,150	0,125
Weight (*g*)	20,062	19,901	2,815	1,262	0,586	0,170
cumulative (*g*)	133,059	152,960	155,775	157,037	157,623	157,793
cumulative (%)	84,325	96,937	98,721	99,521	99,892	100,000
% passing sieve	15,675	3,063	1,279	0,479	0,108	0,000
P (passing)	0,157	0,031	0,013	0,005	0,001	0,000
Gauss value	-1,008	-1,872	-2,233	-2,591	-3,068	

Starting from the largest to the smallest sieve diameter the cumulative mass and the cumulative percentage of the mass are calculated (rows 3 and 4 in the table). From this last value the percentage of mass that passes each sieve can be determined (row 5). These percentages of passing are plotted in a sieve curve on a logarithmic scale, shown in figure5.4. The sieve curve has a characteristic S curve. From this curve you can read the values of the D_{10}, D_{50} and the D_{60}, by looking at the corresponding percentages.

figure 5.4 Sieve curve; sample 1

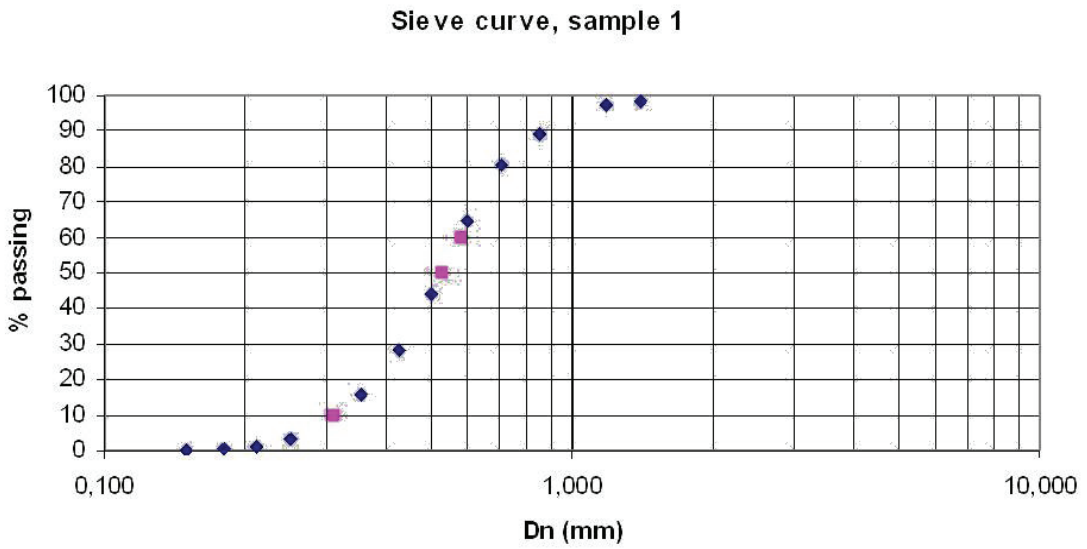

An additional calculation is done, to check the reliability of the results: when plotted on a logarithmic-gauss scale, the results must form a straight line. In order to do so, first the percentage of passing must be translated to a probability of passing (row 6 in the table). From these probabilities the inverse of the cumulative normal distribution function must now be computed. This is done by Excel, the values are shown in row 7 in the table. A new plot in log-gauss scale clearly shows that the results approach a straight line (figure 5.5).

figure 5.5 Sieve curve on a log-gauss scale, sample 1

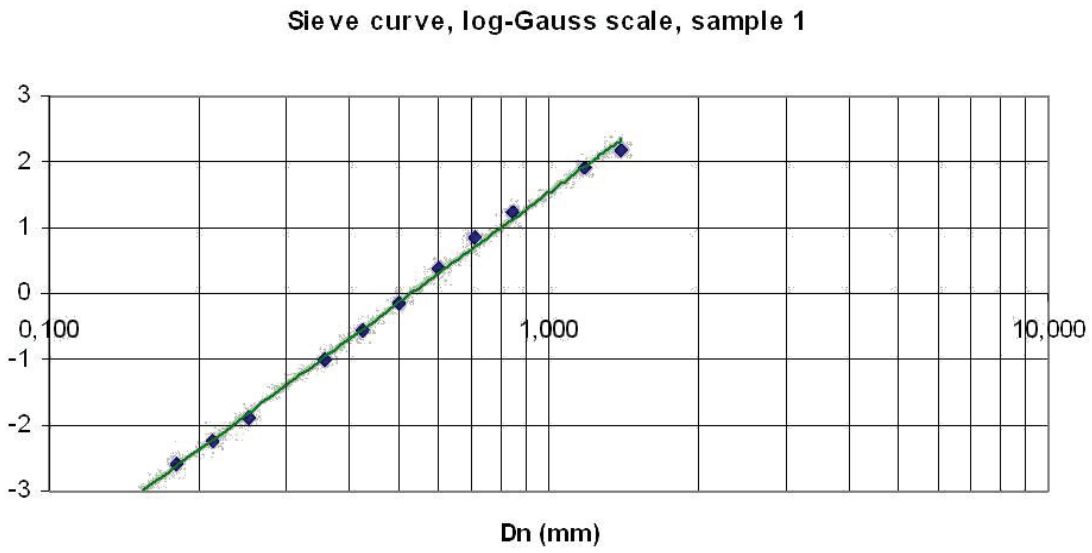

The grading of all samples can be found in appendix V. These results are used for the morphological computations and predictions in chapter 4.

6 Wave analysis

Wave measurements are important for several reasons. The most important reason in this case is to determine what kind of wave climate can be expected for the breakwater and the marina. Wave observations on the other hand, can give you insight in e.g. the bathymetry of the location.

6.1 Wave measurement techniques

Wave measurements and observations have been done in three different ways. The different methods will be treated separately in this chapter.

- Wave height and period measuring, using a pressure meter
- Wave height and period observing, which include observing refraction and diffraction patterns.
- Wave height and period determination, using deep water wave statistics.

Pressure meter

One way to determine wave height is with use of a pressure meter (figure 6.1). A pressure meter measures the difference between a reference pressure, which has been set to the air pressure and the actual pressure measured at a certain level below the water level.

figure 6.1 Pressure meter

figure 6.2 Wave motion in periodic unbroken wave

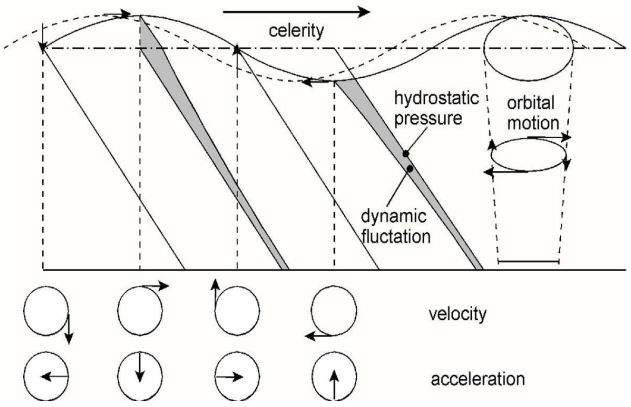

Under a wave, the pressure beneath a crest differs from the pressure beneath a trough, and from this difference a surface elevation can be determined (figure 6.2). To determine the surface elevation, the following equation is used:

$$p = -\rho g z + \rho g \eta \frac{\cosh k(h+z)}{\cosh kh} \sin\theta$$

equation 6.1

p = pressure difference in *kPa*
ρ = water density = 1018 kg/m^3 (reference of Daskalov)
g = gravity acceleration = 9.81 m/s^2
z = depth of the pressure meter beneath undisturbed water level in *m*
η = water elevation in *m*
k = wave number (see appendix VI for determination with the Visser aproximation)
h = water depth *m*
θ = phase function defined as θ = ωt - kx

With sinθ = 1, this becomes for the surface elevation

$$\eta = \frac{(p + \rho g z)}{\rho g} \frac{\cosh kh}{\cosh k(h+z)}$$ equation 6.2

From the surface elevation the wave height can be determined. First the number of zero-downward crossings is counted, to determine the number of waves. Then for every wave the lowest trough and highest crest are determined (figure 6.3).

The absolute value of the lowest trough added with the highest crest give the wave height for each wave.

$$H = |\eta_{min}| + \eta_{max}$$ equation 6.3

After this is done the maximum and minimum wave height, the average wave height & standard deviation and the significant wave height ($H_s = H_{1/3}$) are determined. Finally the wave height distribution is determined.

figure 6.3 Determination of waves

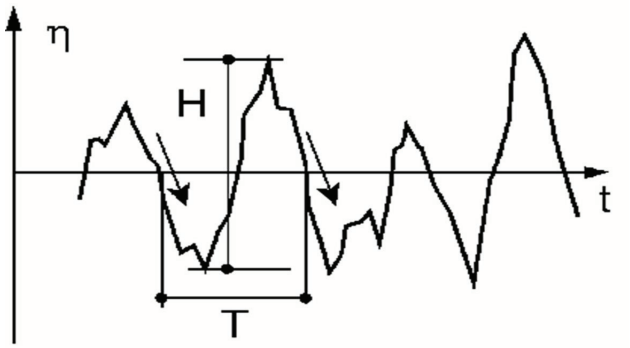

Visual observations

The visual observations took place near the planned breakwater at Byala and at St. Constantin near an area parallel to a jetty. The waves were counted and their height was measured in a fixed number. The waves at Byala were breaking waves, but at St. Constantin they were not.

- Byala

The observations that took place at the breakwater could not give us any information concerning the wave height since there was no reference scale. A total number of 200 waves was observed and recorded in two sets. By dividing the total measuring time with the total number of waves, the average wave period was obtained. Apart from the wave height and period, diffraction, refraction en shoaling patterns were observed and recorded.

- St. Constantin

Concerning the observations near the jetty at St. Constantin, two different measuring locations were chosen. Firstly, 292 waves were recorded at a location parallel to the jetty which was more or less at the same horizontal level and afterwards 200 waves were recorded standing on a hill near the beach in an angle with the jetty. In this way the observations were more accurate.

- Equipment

For the visual observations near the jetty, a theodolite was used. This equipment was used to get a clear view of the wave movement in reference to a ruler, which was tied to the jetty. During one wave period trough and crest were recorded respectively.

Deep water wave statistics

The final method to determine wave height near shore, is using deep water wave statistics. Figure 6.4 shows the average deep water wave height distribution for the Black Sea.

figure 6.4 Wave height exceedance Bulgaria

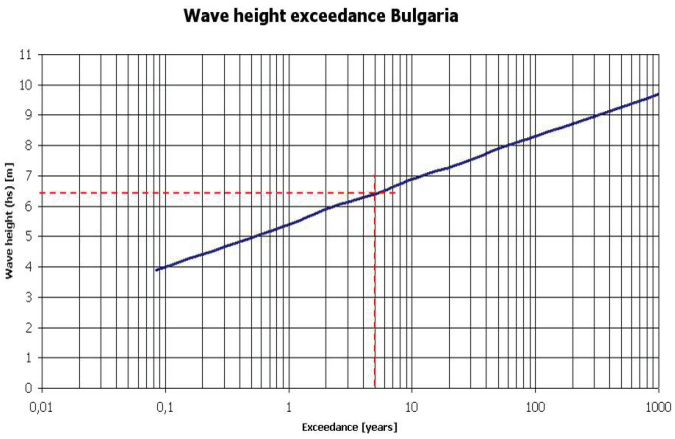

figure 6.5 Distribution deep water wave height

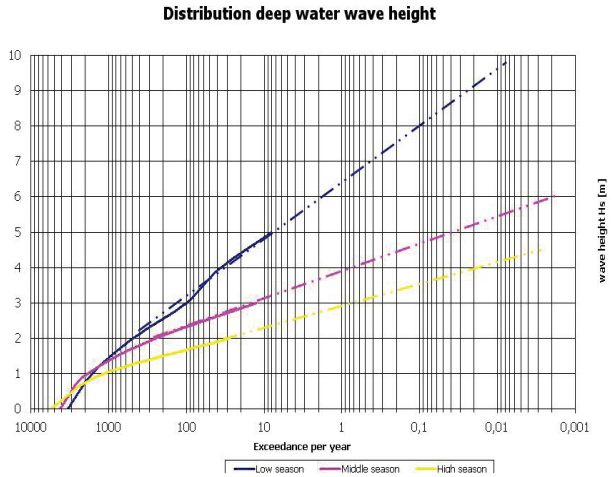

Since for the design of the marina breakwater a difference can be made in boundary conditions during different parts of the year, a seasonal wave height distribution is more valuable. Figure 6.5 shows the seasonal wave height distribution for the Black Sea. From these two graphs, the following wave heights are acquired (table 6.1)

table 6.1 Return period of seasonal and year round wave height and period

return period	1		0,2		0,1		0,01	
	H_s	T	H_s	T	H_s	T	H_s	T
summer	*2,9*	*5,5*			*3,5*	*6*	*4,2*	*6,5*
middle	*3,9*	*6,5*			*4,8*	*7,5*	*5,5*	*8*
winter	*6,4*	*9*			*8*	*10,5*	*9,5*	*12*
year through			*6,6*	*9*				

Notation

H_s = Significant wave height in meters
T = Wave period in seconds

figure 6.6 Depth profile

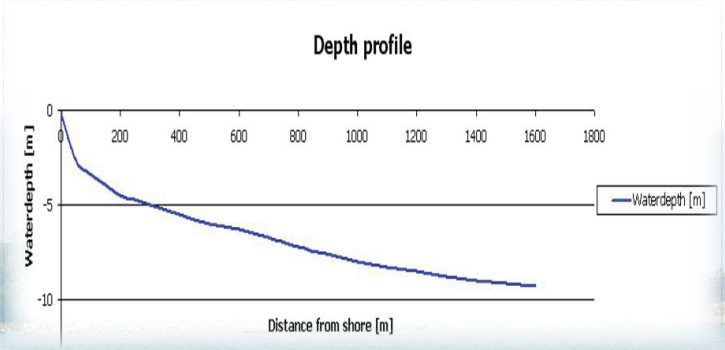

These values along with the depth profile are entered in the program CRESS. Cress then calculated the near shore wave heights for the different seasons and return periods.

6.2 Results

Pressure meter

Two different measurements were done with the pressure meter. The first measurement was done at the breakwater near Byala (figure 6.7).

To make a useful measurement, approximately 100 waves have to pass the pressure meter. From visual observations a wave period of approximately 6 seconds was derived, so the total measuring time should be ten minutes at least. The measurement which was done, lasted more than 17 minutes.

The measurement was done with a time step of 1 second, which means that every second a measurement was done. This resulted in wave data for the breakwater near Byala. The surface elevation is shown in figure 6.8. Important data is given in table 6.2 (see next page).

figure 6.7 Measurements at the breakwater

figure 6.8 Surface elevation at Byala

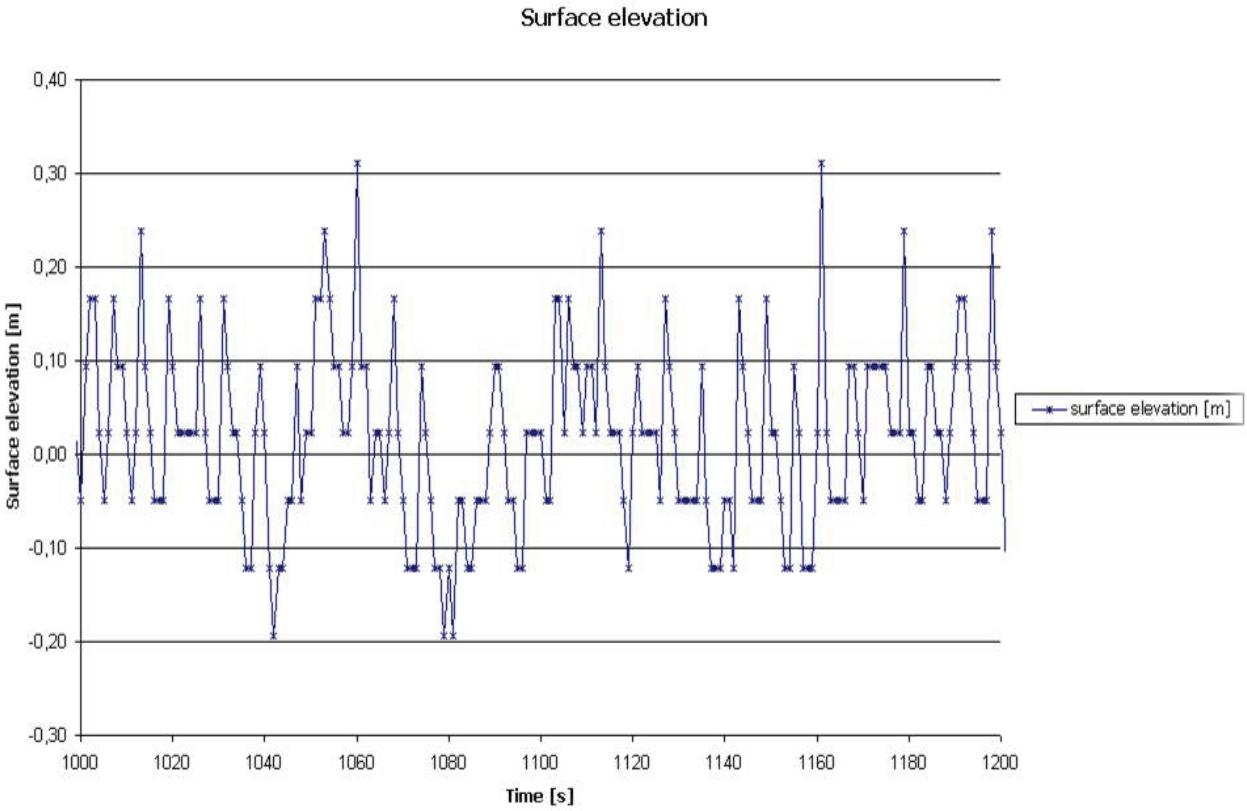

The wave period used here, is determined by dividing the recording time by the number of recorded waves. The following wave characteristics were obtained after calculation. table 6.3 on the next page

table 6.2 Surface elevation data Bayla

Lowest trough	*-0,27*	*m*
Highest crest	*0,31*	*m*
Average surface elevation	*0,00*	*m*
Elapsed time	*17,12*	*min*
Number of waves	*153,00*	*-*
Average wave period	*6,71*	*sec*

table 6.3 Calculated wave characteristics Bayla

Maximum wave height (H_{max})	*0,43*	*m*
Minimum wave height (H_{min})	*0,05*	*m*
Average wave height (H_{avg})	*0,22*	*m*
Standard deviation wave height	*0,08*	*m*
Significant wave height ($H_s = H_{1/3}$)	*0,30*	*m*

The second measurement was done at the jetty near St. Constantin (figure 6.9). The measurement period there was about 29 minutes with a wave period of approximately 4 seconds. This is sufficient to obtain at least 100 waves.

This measurement was done with a time step of 0.1 second, to obtain more data points, so the result would be more accurate.

This yields the following results for the surface elevation, at the jetty near St. Constantin (figure 6.10), some data is given in table 6.4.

figure 6.9 Measurements at the jetty

figure 6.10 Surface elevation at St. Constatin

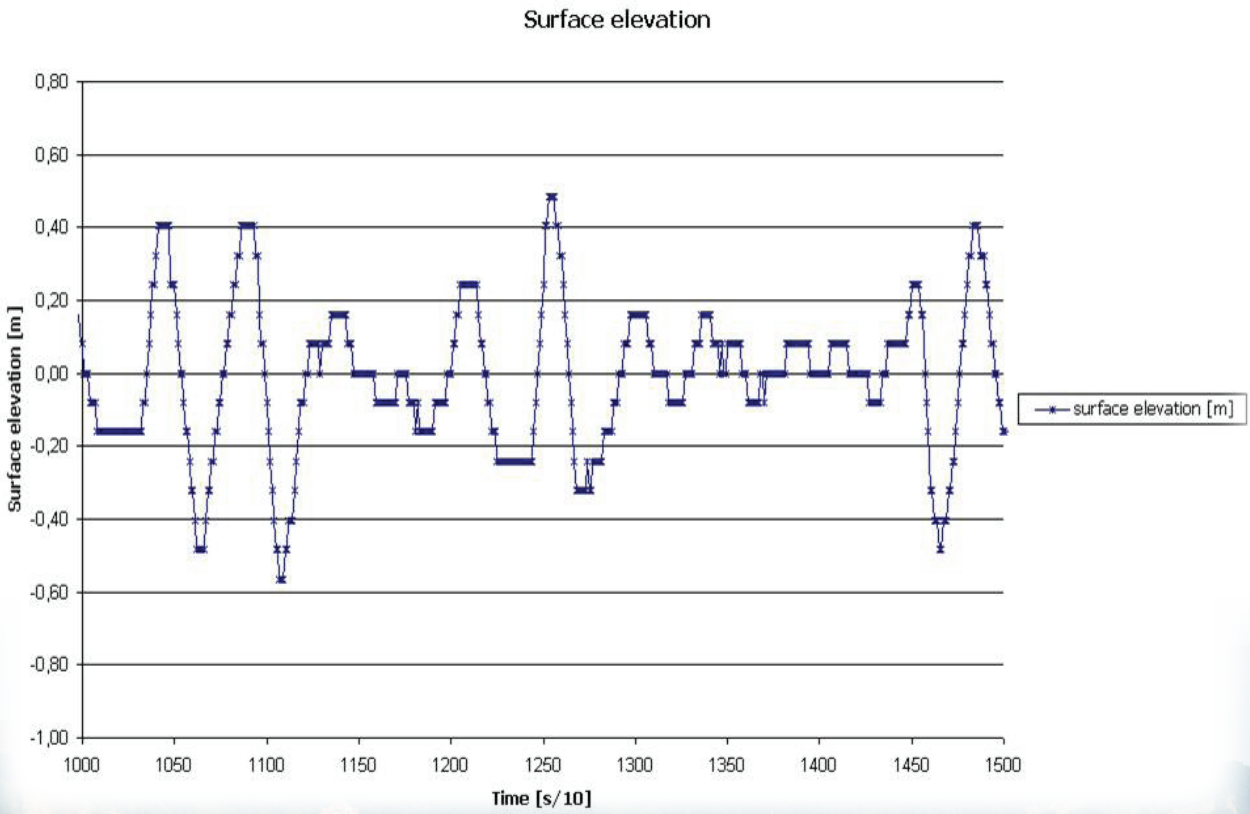

table 6.4 Surface elevation data St. Constantin

Lowest trough	*-0,65*	*m*
Highest crest	*0,57*	*m*
Average surface elevation	*0,00*	*m*
Elapsed time	*28,92*	*min*
Number of waves	*456,00*	-
Average wave period	*3,80*	*sec*

table 6.5 Calculated wave characteristics St. Constantin

Maximum wave height (H_{max})	*1,29*	*m*
Minimum wave height (H_{min})	*0,08*	*m*
Average wave height (H_{avg})	*0,53*	*m*
Standard deviation wave height	*0,26*	*m*
Significant wave height ($H_s = H_{1/3}$)	*0,82*	*m*

The wave period, again, is determined by dividing the recording time by the number of recorded waves. The wave characteristics were obtained after calculation (table 6.5).

The wave characteristics obtained at St. Constantin are used to make a distribution for the wave height, using $H_s \Xi H_{13.5\%}$ $H_{1\%} \approx 1.5H_s$ and $H_{0.1\%} \approx 1.85H_s$ .This yields the distribution graph for the wave height at St. Constantin as in figure6.11.

figure 6.11 Wave height distribution

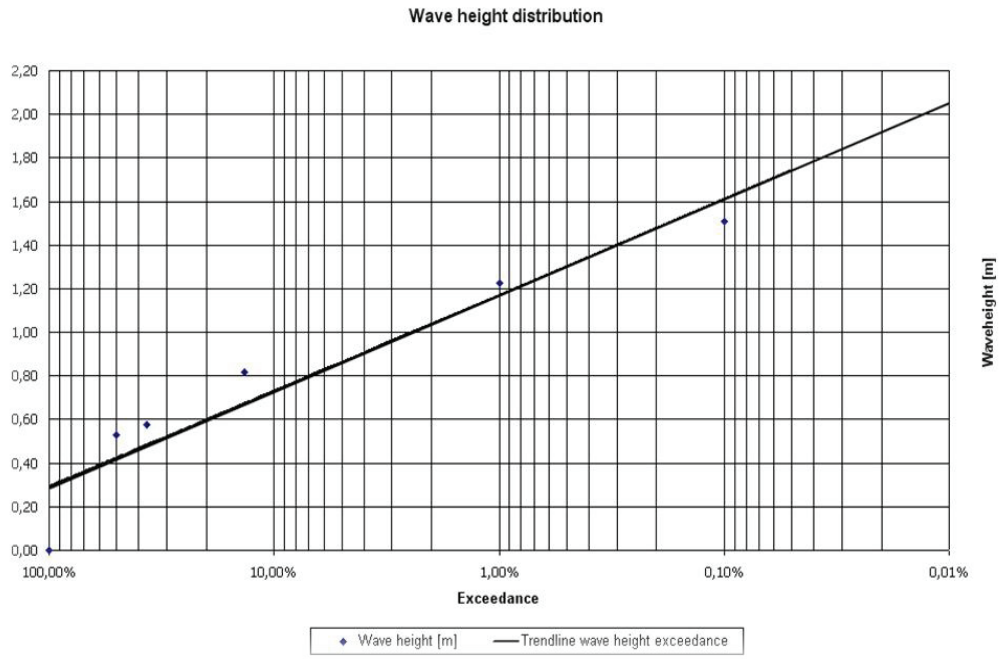

This distribution shows that a wave height of approximately 2.05 *m* has an exceedance of 0.01%.

In both cases the measurements were done very close to a structure, which influences the wave pattern. At the jetty near St. Constantin, this influence is negligible but at Byala, where the measurements were done near the breakwater, the influences are strong.

A more important difference between the two measurements is the time step. Because the time step was set too low at the measurement near Byala, the results become quite inaccurate, because there are approximately only six measuring points per wave. Because of this zero downward crossings could have been missed, and therefore the wave number could easily be to low. Therefore the data from St. Constantin is used to make the distribution.

Finally, in both cases only one measurement was done. To obtain a more accurate wave distribution, several measurements should be done at different moments in time.

Visual observations

The following table (6.6) gives the acquired results from the visual observations, that took place at the tip of the breakwater near Byala.

table 6.6 The observation record of wave period

200 waves categorized in 20 groups of two sets of measurements													
	1	*2*	*3*	*4*	*5*	*6*	*7*	*8*	*9*	*10*	*Average*	*Stand. dev.*	*Period T*
Set 1	*54,3*	*59,4*	*62,1*	*61,0*	*63,8*	*59,9*	*62,3*	*60,8*	*60,8*	*57,0*	*60,49*	*2,75*	*6*
Set 2	*64,7*	*59,3*	*57,2*	*64,1*	*66,8*	*70,6*	*62,8*	*61,9*	*63,0*	*62,9*	*63,38*	*3,71*	*6,3*

Wave diffraction, wave breaking and shoaling were also observed at this location. The waves approach the breakwater in an angle of approximately 50 degrees. Due to the tetrapods of the breakwater the wave reflection was limited.

The wave height near the tip of the breakwater becomes higher and higher, until the waves break. However, the wave height far away from the breakwater does change at all. The height of the breaking waves does not change much. The waves bend around the tip of the breakwater and thus penetrate the lee side of the breakwater. This phenomenon is called diffraction.

The extension line of the breakwater is a distinguished line of the wave height on one side which is much higher than the wave height on the other side. Moreover at the tip of the breakwater the depth is decreased because of the sedimentation. This sedimentation has created a shoal in the protected area of the breakwater, where the waves are breaking.

figure 6.12 Wave interaction with the fisherman's breakwater Byala

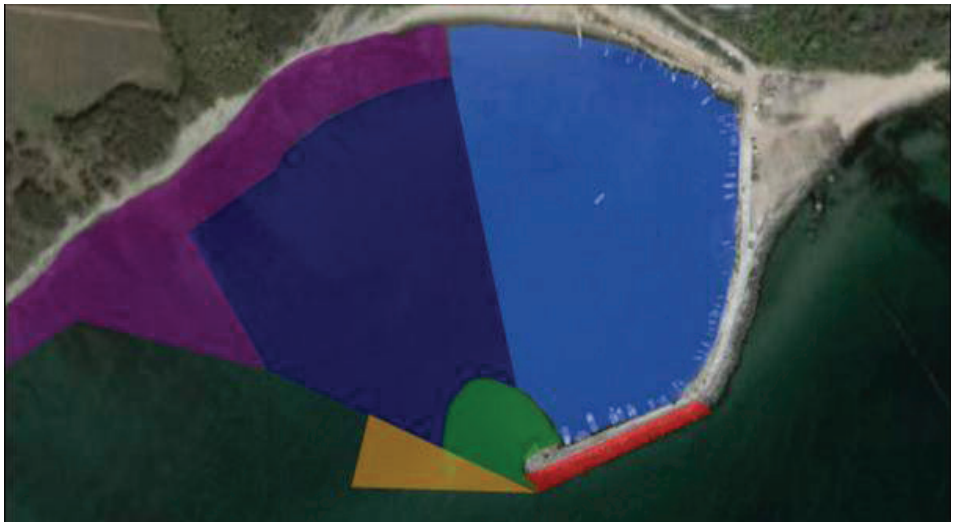

- Red zone: Breaking waves on the breakwater
- Yellow zone: White capping
- Green zone: Breaking waves on the shoal
- Light blue zone: Only local wind induced waves
- Dark blue zone: Low energy waves due to diffraction
- Purple zone: Depth induced surf zone breaking of waves

From the visual observations at St. Constantin the wave height distribution, is derived. This can be seen in figure 6.13.

figure 6.13 Wave height distribution by visual observation

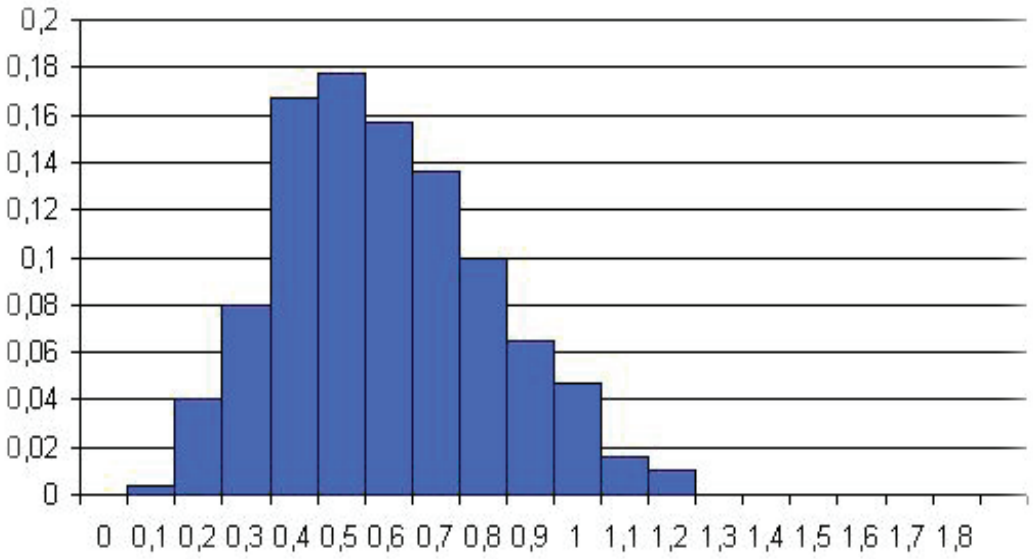

The observed wave heights are divided into 10 categories, ranging from 0.1 to 1.3 meter. After counting the number of waves in each category, the wave distribution is obtained. From this dataset, a significant wave height of H_s = 0.89 *m* has been determined. Using the same method as with the pressure meter, this yields a distribution graph for the wave height at St. Constantin (figure 6.14);

figure 6.14 Wave height distribution from visual observations

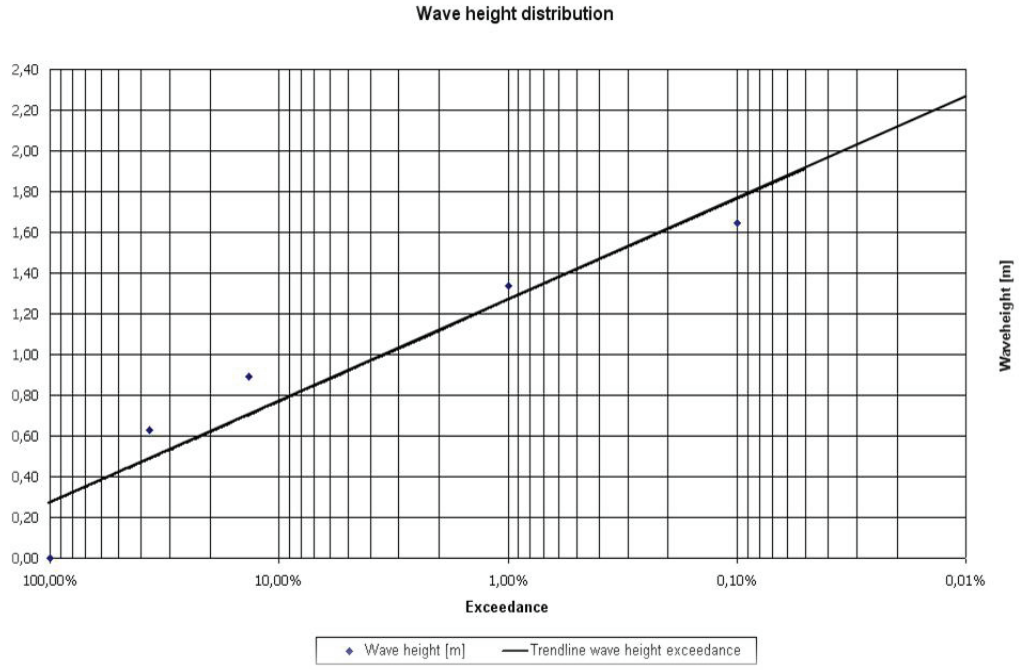

This distribution shows that a wave height of approximately 2. 28 *m* has an exceedance of 0.01%.

Deep water wave statistics

The results calculated by CRESS (appendix IX), give the following values (table 6.7) for the location where the marina breakwater is planned.

table 6.7 Seasonal wave heights at new breakwater location, per return period

Return period once per year

Distance from shore	Waterdepth	H_s summer	H_s middle	H_s winter
155	*-4*	*1,73*	*1,93*	*2,25*

Return period once per 10 year

Distance from shore	Waterdepth	H_s summer	H_s middle	H_s winter
155	*-4*	*1,84*	*2,07*	*2,41*

Return period once per 100 year

Distance from shore	Waterdepth	H_s summer	H_s middle	H_s winter
155	*-4*	*1,94*	*2,14*	*2,56*

Notation
Distance from shore in meters *Waterdepth in meters* *H_s = significant wave heigth in meters*

When all the obtained values are used, the following graph for wave height at a certain distance from shore is obtained. The location of the breakwater is indicated with the red vertical line (figure6.15).

figure 6.15 Seasonal shallow water wave height

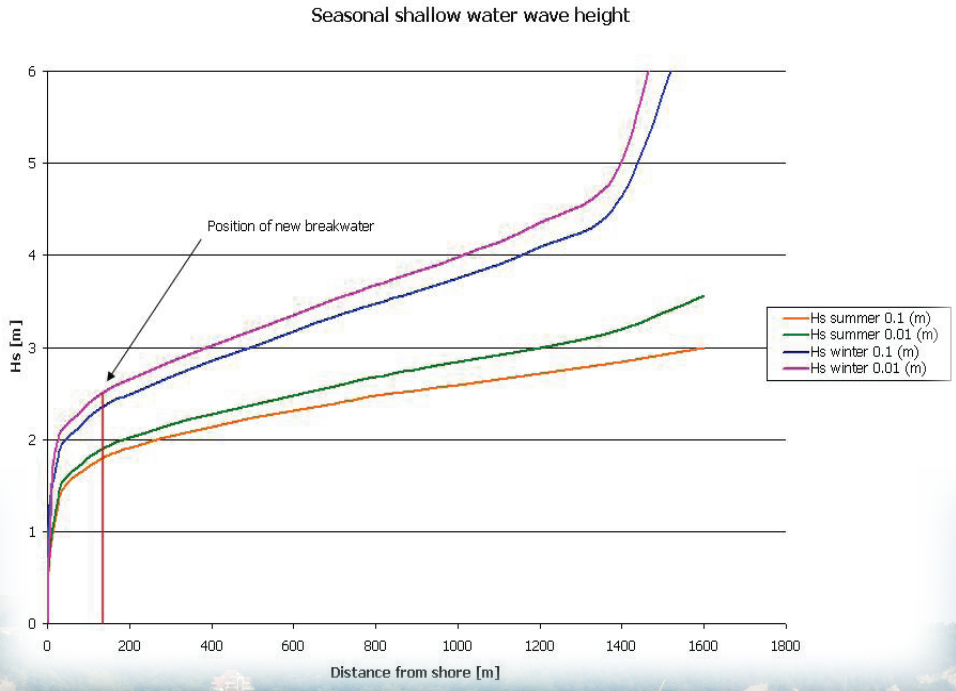

In this graph, wave height for two seasons – summer and winter – and two return periods – 10 and 100 years – are compared. The difference in wave height between the two return periods is, as can be seen, very small for the location of the planned marina, whereas the differences between the wave height calculated for the deeper water condition differ much more.

Another important aspect which can be deducted from these data, is the difference between summer and winter conditions. Since the marina will be empty during the winter season, more wave penetration can be allowed. The breakwater protecting the marina, should only be dimensioned according to the summer wave height conditions, which is approximately 0.6 meter lower.

The average near shore wave height, with a return period of every 100 year, is approximately 2.2 *m*.

6.3 Final conclusions

The first most important conclusion for the two 'measuring' methods (using the pressure meter and visual observations by theodolite) is that in both cases, the measuring time is too short to obtain a desirable amount of data. The data obtained is limited, since they represent only a short timescale and do not cover the wave climate of a complete year. Therefore, these results should not be taken as representative wave heights for the design of a breakwater.

As for the results obtained with the use of deep water wave statistics, its accuracy is questionable. The values used, have been derived from the graphs. The original values, used to make the graphs, were not accessible. Yet, the values obtained with deep water wave statistics are probably the most accurate, because the deep water wave statistics include a wide data range.

Remarkable is that the exceedance values for a return period of 100 years, are very similar for all three methods. For the pressure meter it is 2.05 *m*, for the visual observations it is 2.28 *m* and for the deep water wave statistics it is 2.2 *m*. This similarities might indicate that the obtained values are correct. However the methods used to obtain the data are all very inaccurate. Therefore it is more likely that these similarities are just a coincidence.

Finally, the wave distributions from the two measurements were done at St. Constatin and it is not certain that the wave climate at Byala is the same as the wave climate at St. Constantin.

7 Breakwater

7.1 Existing tetrapod breakwater Byala

The existing tetrapod breakwater has been built in the 1980's. This paragraph assesses the strength of the existing tetrapod breakwater. Primarily the results of the visual inspection will be described. Secondly, the tetrapod characteristics will be calculated followed by a calculation of the design wave. Next, the maximum depth limited wave is calculated and compared with the design wave. Finally, the wave transmission and breakage of the tetrapods are discussed after which a conclusion is drawn.

7.2 Visual Analysis

Tetrapod quality

The concrete of the tetrapods show lots of cracks. The grains are showing at many tetrapods. Still, there are only few tetrapods that are broken. The estimated percentage of broken tetrapods is 0.5%. The estimated number of elements is approximately 5 per meter for the northern half of the breakwater. South of that the intensity is less: about 3,5 ~ 4 per meters. It is also quite clear that the tetrapods with the highest quality are placed near the waterfront and the worst are placed on top and in the back. Two types of tetrapods were used for the breakwater: a smaller type and a bigger type weighing almost twice as much.

The tetrapods are placed on top of a core of rocks with diameters varying from roughly 0.10 *m* to 1.0 *m*. Locally the core material is covered with concrete which has been poured over it on-site. More about the tetrapods is described in the next paragraph.

figure 7.1 Concret grains visible

figure 7.2 Broken tetrapod

Displacement

Over a distance of less than 50 meters at the north end of the breakwater, the tetrapods seem to have been displaced over a few meters. It is hard to tell if they actually have been displaced, or that they where placed here on purpose. The "displacement" occurred at the location where mostly smaller tetrapods were present. The smaller core material has become visible and therefore relatively unprotected. Small rocks from underneath the quay have been washed away. So far this undermining has not led to failure of the quay.

Water circulation pipes

At approximately 90 *m* south of the beginning of the breakwater, two pipes (d≈ 1 *m*) used to run under the breakwater. These pipes were constructed here to assure water circulation inside the port basin. One of the pipes was already completely deteriorated at the inner side of the breakwater. Only the steel reinforcement, rubble material and core material remained. Blockage of the core material in the pipe is the reason for this failing.

Also, the second pipe underneath the quay has an opening between the elements due to settling. This caused a fountain of water bursting up underneath the quay after each incoming wave (water hammer). This way the pipe directly transfers the wave energy into the core of the breakwater, which has led to external movement of core material. However, this undermining seems stable and has not yet caused severe damage of the quay, since the remaining rock material is too big to be washed out.

figure 7.3 Opening between pipe-elements

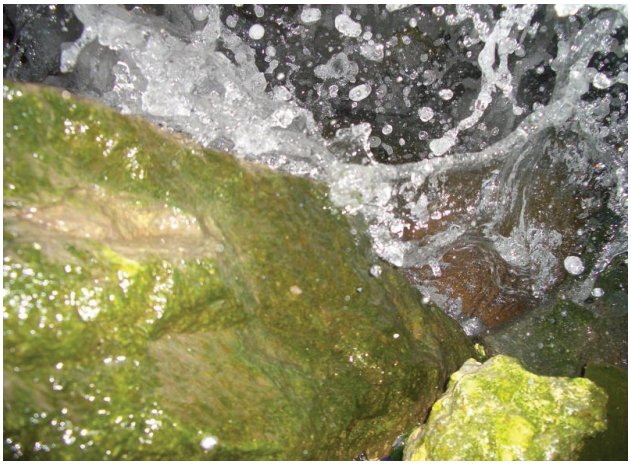

figure 7.4 Water from the incoming wave underneath the quay

The use of low-pressure sewer pipes instead of high pressure pipes seems quite relevant for this situation. Also the entrance of the pipes should have been situated deeper and in front, instead of within the breakwater

The inspection revealed signs of past maintenance of the breakwater itself. The original breakwater was constructed in the eighties. Nevertheless, different dates e.g. 1994 and 1998) were spotted on some of the tetrapods placed on top of the breakwater, which probably refer to the year they were constructed. A plausible explanation is that at the end of the nineties some extra tetrapods were placed to fill up empty spots caused by downward settled tetrapods.

Over a long stretch at the inner side of the breakwater, the quay has been reinforced with rip-rap. This is not very practical considering the fact that ships have to moor here. In the original plans a second breakwater was designed south of the bay. This to combat effects of diffracting and refracting waves. This breakwater was never build however.

figure 7.5 Rip rap reinforcement

Apart from the unprotected core material over a stretch of approximately 50 *m*, the condition of the breakwater is quite good. In the following paragraphs several calculations have been made to further assess the breakwater strength and review the design criteria at the time of construction.

figure 7.6 Slope angle of tetrapods

figure 7.7 Tetrapod breakwater

7.3 Tetrapod analysis (Primary armour layer)

From measurements it was derived that there are two types of tetrapods used for the breakwater. Some of the characteristic dimensions are shown in figure 7.8. With the volume was calculated. The specific density of the concrete was determined to be 2230 *kg/m*³. Thus, the weight of the tetrapods could be calculated. The smaller tetrapod (type 1), has a weight of 3000 *kg*, the larger one (type 2) is more than twice as heavy, having a weight of 6600 *kg*.

figure 7.8 Characteristics of a tetrapod

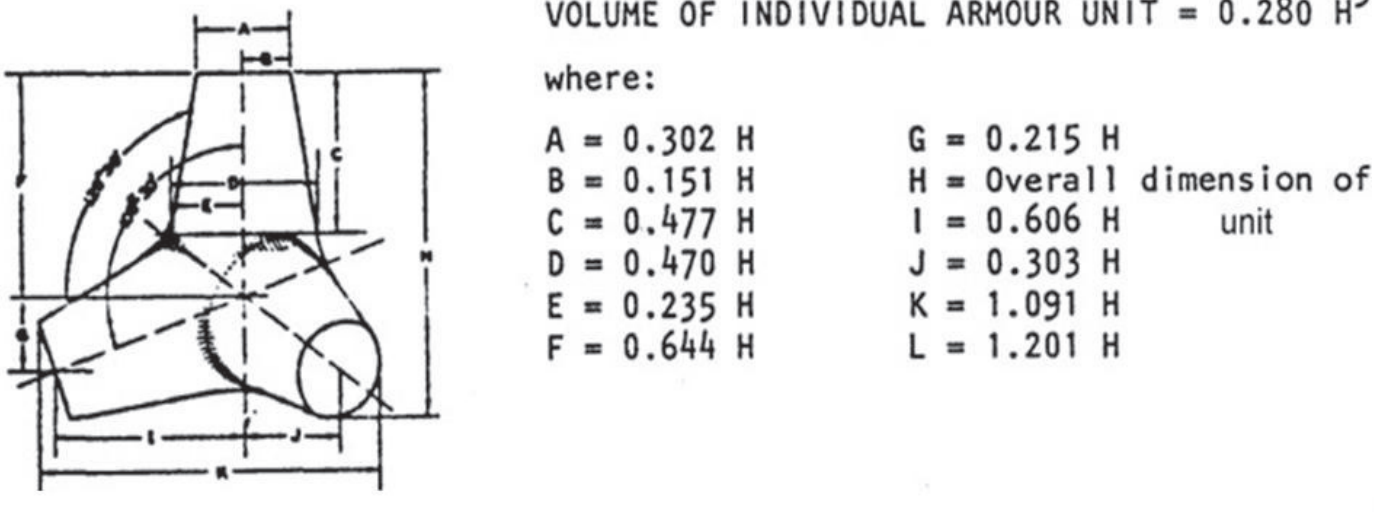

The smaller tetrapod has mainly been used over the first 60 *m* with a gap of 20 *m* in between at the location where some concrete caissons are present. From 60 *m* on, the larger type has been used. None of the tetrapods has steel reinforcement as could be seen from the broken elements. The tetrapods have been placed under a slope ranging between 1:1 and 1:1.7. The placement of the tetrapods is displayed in the figure 7.6.

7.4 Breakwater design-wave analysis

With the parameters from the previous paragraph, the design wave (H_s) can be calculated. For this purpose three calculation methods have been used, namely: Van der Meer, Hudson and Hanzawa. The results of the different methods are displayed at the end of this paragraph.

Hudson

Apart from the relative density and the element diameter, the method of Hudson takes the slope and a damage factor into account, as can be seen in the equation 7.1:

$$\frac{H_{sr}}{\Delta d} = \sqrt[3]{K_d \cot \alpha}$$ equation 7.1

The slope varies between 30° and 45° (cot(α)=1.7 and cot(α)=1). But since the value is taken to the power 1/3, the influence is relatively small. Still, the steepest slope is taken to be normative. For the head of the breakwater K_D=5 for breaking and K_D=6 for non breaking waves. In this case 5 is chosen to be normative.

The Hudson formula is simple, but has therefore also a few shortcomings. Primarily, the wave period is not in the formula. Secondly, Hudson assumes permeable breakwaters. A method that does account for these important parameters is the Van der Meer method.

Hanzawa

The method of Hanzawa accounts for both the size of the storm (number of waves N) and the damage, N_{od}. Furthermore, it applies especially to tetrapod breakwaters. Still, the wave period is absent. The formula is typically for slopes of approximately 1:1.5, which is actually shallower than on some parts of the Byala breakwater. The formula is shown as equation 7.2.

$$\frac{H_s}{\Delta D_n} = 2.32\left(\frac{N_{od}}{N_z^{0.5}}\right)^{0.2} + 1.33$$ equation 7.2

Van der Meer

The method of Van der Meer distinguishes between surging and plunging waves. For the current situation at Byala, both wave types can occur. This is because of the varying slope. The two formulas are shown below (equation 7.3.1 and equation 7.3.2):

$$\frac{H_s}{\Delta D_n} = \left(8.6\left(\frac{N_{od}}{\sqrt{N}}\right)^{0.5} + 3.94\right)s_m^{0.2}$$ (plunging breaker) equation 7.3.1

$$\frac{H_s}{\Delta D_n} = \left(3.75\left(\frac{N_{od}}{\sqrt{N}}\right)^{0.5} + 0.85\right)s_m^{-0.2}$$ (suring breaker) equation 7.3.2

The D_n in the calculation is the length of a cube with the same weight as the tetrapod. Δ is the relative density of the tetrapods which can be calculated from the water and concrete density. For the calculation also a number of parameters have been estimated. The parameter N_{od} is a damage factor which indicates the number of units displaced out of the armour layer within a strip with the width of D_n. Since this is difficult to see at the location, the value is set to the lower boundary, N_{0d}=0.2, which means that only little damage is allowed. The parameter N stands for the number of waves of the storm this can be calculated from the storm duration and the mean wave period. Since the former is not exactly known, N is approximated by 7500. These approximations of N_{od} and N are acceptable while their influence in the equation is relatively small (they are taken to the power 0.5 and 0.25 respectively). The last parameter in the equation is s_m, which is the wave steepness of the mean deep water wave. It is assumed that the normative storm consists mostly of wind waves. This value is approximated by 0.05 which is the steepness of wind waves. This value is also of small influence while it is taken to the power 0.2 or -0.2 depending on the Irribarren number.

Calculation Results

The results of these calculations are incorporated in appendix X . A summarized overview is given in the table 7.1. It becomes apparent that the Hudson formula displays the most conservative results. As said before, it is also clear that there is a significant difference between the plunging and surging wave results for the Van der Meer method. Hanzawa displays values that are roughly in between those of Van der Meer.

table 7.1 Summerized overview calculated wave heigth

Tetrapod type	Hudson	Van der Meer		Hanzawa
		plunging (ξ < 3)	surging (ξ > 3)	
Type 1	*2.30*	*3.22*	*2.52*	*2.72*
Type 2	*3.00*	*4.19*	*3.29*	*3.78*

Notation
H_s = *significant wave heigth in meters*

To be secure, the Van der Meer results of the surging wave situation are preferable above those of the plunging situation. The results of Hudson are most likely an underestimation of the breakwater strength because the method fails to incorporate some important parameters. Hanzawa is typically for slopes of 1:1.5 while the slopes at the breakwater are steeper at some places. Therefore, the design wave height used for the Byala breakwater is assumed to be approximated best by using Van der Meer (surging waves). With wave heights of 2.52 *m* for type 1 and 3.29 *m* for type 2 tetrapods.

7.5 Maximum depth-limited wave

During visual inspection of the tetrapod breakwater, that over a large stretch the waves were breaking before they reached the breakwater. This means that the wave height is limited by the local depth in front of the breakwater. Below, a detail of the depth chart is displayed. It is visible that this is the case in front of the breakwater (figure 7.9).

At 50 meter from the breakwater, the depth is even less than 4 *m*. A quick calculation according to the depth limited wave calculation, shows that at this location the wave height is already limited to approximately 0.6*4 = 2.4 *m*. At the northern end of the breakwater the smaller tetrapods are located. Here, the depth is even more limited, as the -4 *m* depth contour runs at a distance of over 100 *m* from the breakwater (figure 7.10). It is therefore physically not possible that the earlier calculated design wave will actually reach the breakwater. During a storm, wind setup can lead to higher depths. Breaking of waves is very well be possible then at the tetrapod breakwater.

figure 7.9 Wave breaking in front of breakwater

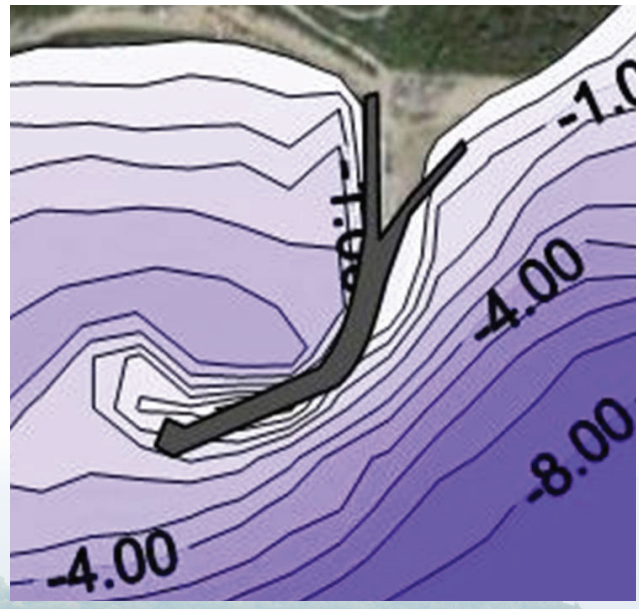

figure 7.10 Depth contours near the breakwater

7.6 Wave transmission

The wave transmission will be analyzed according to CUR 169 guidelines. The wave transmission depends mainly on the relative crest freeboard compared to the wave height. (R_c/H_s). Although this method is a first estimate it gives a good insight into the wave transmission.

figure 7.11 Wave transmission as a function of the relative crest height

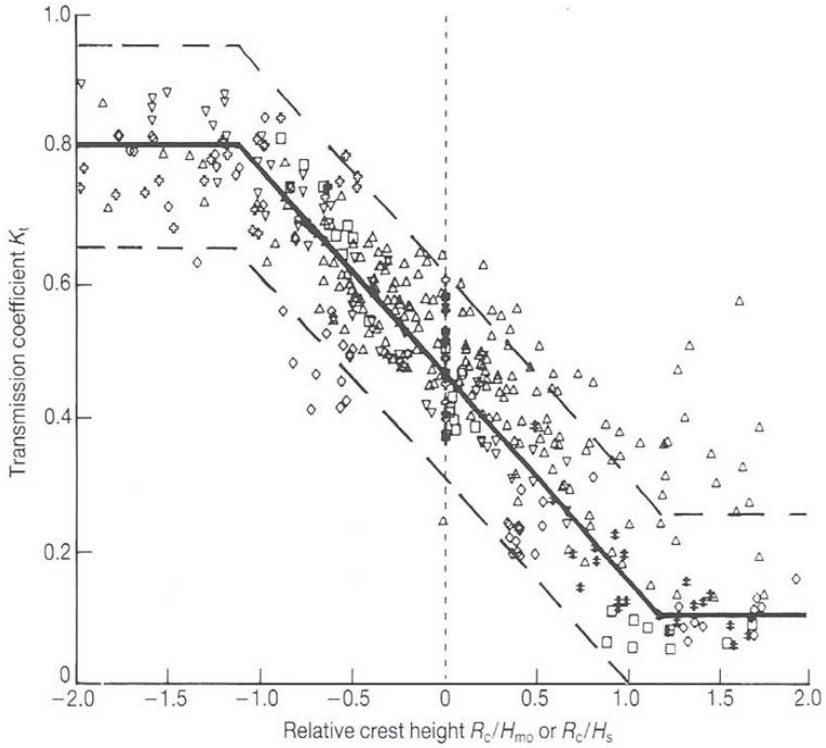

Suppose a maximum wave height of H_s= 2.5 meters. With a crest height of 3.0 *m* the relative crest height becomes 1.20 meters. From figure 7.11 it can be concluded the transmission coefficient is 0.1. This means that the maximum wave height behind the breakwater will be around 0.25 *m*

It is very likely that figure 7.11 can not be applied for relative crest heights and that the transmission coefficient K is much lower. Therefore it can be concluded that the wave height due to transmission is between 0 and 0.24 meters.

7.7 Breakage of the tetrapods

Introduction

In some cases it is possible to determine the wave attack in the past by analyzing the number of broken Tetrapods. For this purpose a calculation is compared with visual observation. The comparison is *Observed percentage of broken Tetrapods* versus *Calculated percentage of broken Tetrapods*.

Calculation

A calculation is been made for the existing breakwater. The method is based on "Empirical formula for breakage of Dolosse and Tetrapods " and is shown in appendix XI. The results are shown in table 7.2.

table 7.2 Calculated percentage of damage on tetrapods

Damage for H_s = 2.5 *m*	
Type 1 tetrapods	
B(5 % upper limit)	1.19 percent
B(5 % lower limit)	0.49 percent
Type 2 tetrapods	
B(5 % upper limit)	0.64 percent
B(5 % lower limit)	0.26 percent

Damage for H_s = 2.0 *m*	
Type 1 tetrapods	
B(5 % upper limit)	0.50 percent
B(5 % lower limit)	0.21 percent
Type 2 tetrapods	
B(5 % upper limit)	0.27 percent
B(5 % lower limit)	0.11 percent

Notation
B = percentage of broken tetrapods

Observations

The observed percentage of broken tetrapods is 0.5 percent. It has to be remarked that there is no distinction in tetrapods that are broken during construction and tetrapods that are broken during severe wave attack.

The conclusion that can be made that the tetrapods that are broken during wave attack, is between 0 and 0.5 percent.

Conclusions

It is very likely that the cause of the broken Tetrapods is construction error. With this assumption one can conclude that no tetrapods are damaged during severe wave attack. Also since it is highly unlikely that a wave higher than 2.5 meters has ever occurred during the lifetime of the breakwater.

7.8 Comparison and conclusions

From the previous it can be concluded that the existing tetrapod breakwater in Byala is over dimensioned. Calculations show that the design wave the breakwater can withstand is unable to reach the breakwater during normal conditions, because of the shallow water depth. The visual observation and breakage calculations also point into this direction. The fact that the tetrapods are constructed of poor quality concrete doesn't have any significant negative consequences since their size compensates for that.

8 Rubble Mound Breakwater Marina

8.1 Breakwater design-wave

For the rubble mound breakwater a preliminary design will be presented. This design is based on preliminary boundary conditions. First, the boundary conditions (the breakwater design wave) will be presented. Following from this, the rock size and the crest height will be determined.

8.2 Breakwater design-wave

The design wave height is the once every five years significant wave height, which is determined in chapter 6. A distinction is made between the summer and winter significant wave height. The winter wave height is characteristic for the ultimate limit state with respect to damage to the breakwater. The summer wave height mainly determines the serviceability limit state through wave transmission and overtopping. The significant wave heights are:

H_s, winter = 2.5 *m*

H_s, summer = 1.8 *m*

8.3 Rock size

For determining the D_{n50} for the breakwater, winter wave height will be taken into account (H_s= 2.5 *m*). According to the Rock Manual the nominal diameter can be calculated from the formula for dynamically stable structures , in which

$$D_{n50} = \frac{H_s}{\Delta N_s}$$ equation 8.1

H_s = significant wave height (*m*)

Δ = relative buoyant density (-)

N_s= Stability number (-)

With a slope of 1:2 and Δ= 1.4, this will result in a nominal diameter of 0.9 meters. The median weight (W_{50}) will therefore be around 1700 *kg* which makes a need for stones of class of 1 to 3 tons.

table 8.1 Mobility parameter

Regime	N_s = Ho	HoTo
Little movement; non reshaping	*<1.5 - 2*	*<20 - 40*
Limited movement during reshaping; statically stable	*1.5 - 2.7*	*20 - 40*
Relevant movement, reshaping; dynamicly stable	*> 2.7*	*> 70*

Notation

The criteria depend to some extend on the rock gradation

8.4 Overtopping

The Rock Manual also has guidelines for determining the amount of overtopping. Just behind the breakwater only the largest vessels should be positioned due to the draught. Since no walking is allowed on the breakwater, table 8.2 allows an overtopping of 50 *liters/s/m*.

table 8.2 Critical overtopping discharges and volumes (Allsop *et al*, 2005)

	q mean overtopping discharge	**V_{max} peak overtopping volume**
Marina		
Sinking of small boats set 5 - 10 *m* from wall, damage to larger yachts	*q > 0.01*	V_{max} *> 1 - 10*
Significant damage or sinking of larger yachts	*q > 0.05*	V_{max} *> 5- 50*

Notation
q = m³/s per m
V_{max}= *m³ per m*

According to Owen the next set of formulas allow estimating the mean overtopping discharges over smooth slopes:

$$R^* = R_c / (T_m (g H_s)^{0.5})$$

$$Q^* = a \exp(-b R^* / g)$$

$$q = Q^* (T_m g H_s) \qquad \text{equation 8.2}$$

A rubble mound breakwater gives a roughness reduction factor (γ) of 0.55. According to the maximum overtopping criterion of 50 *liters/s/m*, a crest freeboard of the breakwater of 2 *m* in combination with 0.5 *m* set-up is found. This gives a freeboard of 2.5 *m* +MSL. In this case the summer wave height is used, since overtopping is only important for this period of year.

8.5 Wave transmission

For small low-crested rubble mound breakwaters the coefficient of wave transmission can be calculated using:

$$C_t = -0.4 R_c / H_s + 0.64 (B / H_s)^{-0.31} (1 - e^{-0.5 \xi_p}) \qquad \text{equation 8.3}$$

R_c = Crest freeboard
H_s = Significant wave height
B = Crest width
ξ_p = Surf similarity parameter

Also in this case only summer conditions are relevant. The transmitted wave criterion (H_t) specified by the contractor is 0.25 meter. However, with $H_t = H_i * C_t$ one can show that no wave transmission should be expected for these conditions.

8.6 Overview

In Figure 8.1 an overview of the calculated results is shown. It includes the requested dimensions and stone size. Also the relevant wave height conditions are provided.

figure 8.1 Simplified result of the new rubble mound breakwater of the marina

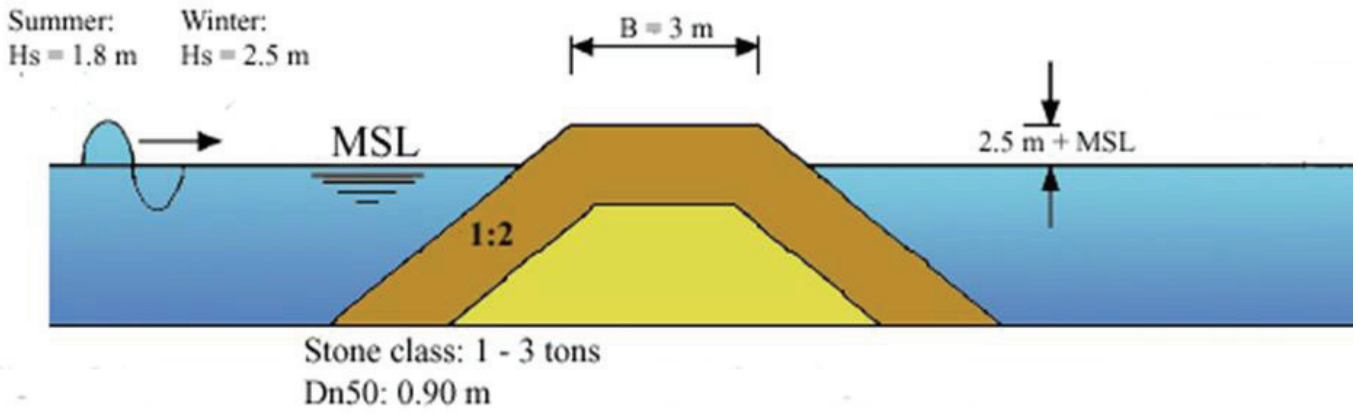

8.7 Level II Calculation

In a probabilistic analysis, different uncertainties in the calculations can be taken into account. The used depth limited wave height used in the previous calculations is defined as $H_{sb} = 0.56*d_b*e^{3.5m}$ according to Kamphuis (1998). With m = 0.02 this becomes $H_{des} = 0.6*d_b$. Increasing water level due to wave setup changes the depth of the water at the structure into the modified depth $d_s' = d_s + 0.1H_{sb}$

Kamphuis also stated that due to the frequent occurrence of design waves and cumulative damage behavior of rubble mound breakwaters, one might consider a zero damage cumulative damage formula. This includes the maximum wave height factor K_{max}, which is determined to be 1,5.

For Byala, both the latter two approaches have been examined, H_{des}= 1,95 *m* and 2,9 *m* with both rock and two qualities of tetrapods. Also a distinction has been made between a Level I and II analysis. The Hudson formula forms the basis of the calculations and takes the influence of the uncertainties of several of its parameters into account. Since the water depth in front of the structure is quite the same for the existing and to be build breakwater, the probabilistic analysis can be used for both scenarios.

It shows that improving the quality of concrete, the total amount of elements to be used can be reduced with 40 percent. According to the desired level of certainty or level of uncertainty in parameters, the required mass of the elements is calculated. In appendix IVX the probabilistic analysis of the rubble mound breakwaters is shown.

9 Rockmaterial for a breakwater

9.1 Supplying rocks from the Martsiana quarry

In order to check whether good quality rock was available for building a breakwater in the neighborhood of the project one quarry was investigated and some parameters of the rock available for hydraulic engineering were checked.

The quarry investigated was a limestone quarry which main production was dust for paint, glass and additives in food production as well as blocks for (rail-)road foundations. The way the quarry is operated in order to produce the several sorts of dust is discussed in appendix XV on the quarry operation. In the quarry large blocks suitable for hydraulic engineering are separated. Some of these blocks are shown in picture 8.1 on the right. These blocks are further investigated. For hydraulic engineering purposes it is needed to determine the D_{n50}, elongation and blockiness, since these parameters can be used in breakwater design. The need for the D_{n50} is clear from the known stability formulae, elongation and blockiness are needed to determine the void porosity in the placed blocks (Newberry *et al.*, 2002) and they could with this void porosity also be used to adapt some coefficients in the Van der Meer equations to make it usable for non-standard blockiness and elongation values (Stewart *et al.*, 2002).

figure 9.1 Sample of investigated rocks

9.2 Quality of the rocks

The D_{n50} can easily be determined if the weight of a given set of rocks is measured and the density of the rock is determined. Therefore the weight was measured of a set of 29 rocks and the density of a sample was measured in the laboratory. The d_n of every stone was determined by the following simple formula:

$$d_n = \sqrt[3]{V} = \sqrt[3]{M/\rho} \qquad \text{equation 9.1}$$

All of these d_n are then drawn on a log-gauss scale, and the D_{n50} could be determined. Elongation, sometimes also called aspect ratio, is defined in CUR manual 154 as:

$$l/d = \frac{longest\ axial\ length}{shortest\ axial\ length} \qquad \text{equation 9.2}$$

Therefore from four of the blocks the longest and shortest axial lengths are measured in order to determine the elongation. Blockiness is defined in CUR manual 154 as:

$$BLx = \frac{Volume}{XYZ} * 100\% \qquad \text{equation 9.3}$$

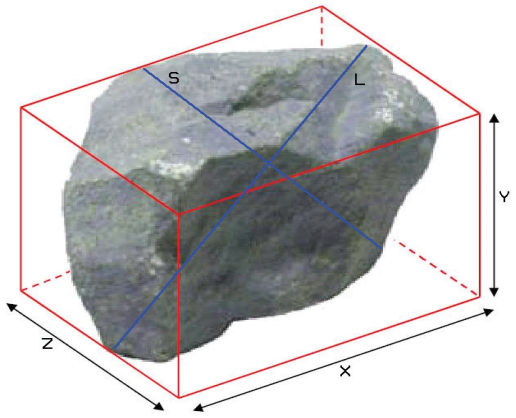

figure 9.2 Stone lengths needed for elongation and blockiness

For that reason the same four blocks as used for the elongation were used to measure values for X, Y and Z. How the lengths l, d (or S), X, Y and Z are determined is shown in figure 9.2.

The void porosity and the layer thickness in breakwaters can be determined using the mean blockiness, the standard deviation of the blockiness and the mean elongation. Newberry *et al.* (2002) propose the following of equations which can be found on the next page in table 9.1.

figure 9.3 Rock measurement

figure 9.4 Quarring rock

table 9.1 Determination of void porosity and layer thickness by Newberry *et al.* (2002)

Double layers
Void porosity
$n_v = 42.38-0.2177\ BL_{cm} + 3.695\ l/d_m - 0.4128\ BLc_{sd}$ {α=1:1.5} $n_v = 42.90-0.2204\ BL_{cm} + 3.740\ l/d_m - 0.4179\ BLc_{sd}$ {α=1:2} $n_v = 43.46-0.2233\ BL_{cm} + 3.789\ l/d_m - 0.4233\ BLc_{sd}$ {α=1:3}
Layer thickness
$k_t = 1.1375+0.0026\ BL_{cm} - 0.1588\ l/d_m - 0.0003\ BLc_{sd}$ {α=1:1.5} $k_t = 1.0736+0.0024\ BL_{cm} - 0.1499\ l/d_m - 0.0003\ BLc_{sd}$ {α=1:2} $k_t = 1.1038+0.0025\ BL_{cm} - 0.1541\ l/d_m - 0.0003\ BLc_{sd}$ {α=1:3}
Single layer
Void porosity
$n_v = 34.53-0.2137\ BL_{cm} + 3.446\ l/d_m + 0.1852\ BLc_{sd}$ {α=1:1.5} $n_v = 35.94-0.2224\ BL_{cm} + 3.586\ l/d_m + 0.1928\ BLc_{sd}$ {α=1:2} $n_v = 36.20-0.2240\ BL_{cm} + 3.613\ l/d_m + 0.1942\ BLc_{sd}$ {α=1:3}

Notation	
BL_{cm} = mean of blockiness coefficients	l/d_m = mean of aspect ratios
BLc_{sd} = standard deviation of blockiness coefficients	α = slope angle

The blockiness and elongation can also be used to refine the stability parameters C_{pl} and C_{su} in Van der Meer's stability equations. Stewart *et al.* (2002) propose the following table 9.2 to adapt these two parameters.

table 9.2 Determination of C_{pl} and C_{su} proposed by Stewart *et al.* (2002)

BLc-range	l/d range	Armour Porosity (%)	Placement method	C_{pl}	C_{su}
40%-50%	1.3 - 3.0	*38.7*	*standard*	*7.09*	-
40%-50%	1.3 - 3.0	*36.1*	*dense*	*6.68*	*1.67*
50%-60%	1.3 - 3.0	*37.1*	*standard*	*6.44*	*1.51*
50%-60%	1.3 - 3.0	*35.2*	*dense*	*7.12*	*2.08*
60%-70%	1.3 - 3.0	*35.5*	*standard*	*7.71*	*2.63*
60%-70%	1.3 - 3.0	*34.4*	*dense*	*10.85*	-
50%-60%	1.0 - 2.0	*36.1*	*standard*	*8.50*	*1.45*
50%-60%	1.0 - 2.0	*34.6*	*dense*	*8.80*	-

Finally the results of the abovementioned measurements and calculations are deployed in an example calculation of a breakwater using the rocks from this quarry. The Van der Meer's stability equations are used for that. For completeness sake these are reproduced here (Schiereck, 2001).

$$\frac{H_s}{\Delta D_{n50}} = C_{pl} P^{0.18} \left(\frac{S_d}{\sqrt{N}}\right)^{0.2} \xi^{-0.5} \qquad \text{(plunging breaker)} \qquad \text{equation 9.4.1}$$

$$\frac{H_s}{\Delta D_{n50}} = C_{su} P^{-0.13} \left(\frac{S_d}{\sqrt{N}}\right)^{0.2} \xi^{P} \sqrt{\cot \alpha} \qquad \text{(suring breaker)} \qquad \text{equation 9.4.2}$$

Given $\xi = \frac{\tan \alpha}{\sqrt{s}}$ and $s = \frac{2\pi H}{gT^2}$. The transition betweens plunging and surging takes place at:

$$\xi_{transition} = \left[6.2 P^{0.31} \sqrt{\tan \alpha}\right]^{\left(\frac{1}{P+0.5}\right)}$$

9.3 Results and conclusions

In appendix XVI on the measurement results a clear overview is given of the values of all 29 weight measurements and of 4 length measurements taken of the rock available.

The density of the rock was determined of one sample to be 710 *g* divided by 295 *ml* meaning about 2400 *kg/m3*. This is quite higher than the expected 2300 *kg/m3* that was said by the operators to be normal for this limestone quarry. In general Bulgarian limestone has a density around 2310 *kg/m3* so the value that is calculated with is this 2310 *kg/m3*.

With this density the d_n of every measured rock could be determined. This d_n is presented in the appendix on the measurement results. Here the resulting graph is presented on log-Gauss paper as figure 9.5, in order to determine the D_{n50}. The resulting D_{n50} is estimated to be 0,59 *m*.

For the elongation and the blockiness the parameters are determined to be as given in table 9.3. The void porosity parameters follow directly from applying the given formulae and are shown in table 9.4.

table 9.3 Elongation and blockiness results

Number	Elongation (-)	Blockiness (-)
1	3,846	*0,608*
5	2,813	*0,536*
9	2,600	*0,547*
14	2,143	*0,739*
mean	2,850	0,608
st. deviation	0,720	0,093

table 9.4 Calculated porosity parameters

Parameter	Slope	Value
Single layer porosity n_v	1:1.5 1:2 1:3	52,22 52,86 53,55
Single layer thickness k_t	1:1.5 1:2 1:3	0,71 0,67 0,69
Double layer porosity n_v	1:1.5 1:2 1:3	43,76 45,53 45,87

As an example here a short calaculation is given of a possible design made with Van der Meer for a breakwater at the marina site. The values used are the given Hs of 2.5 m and Ts of 7 s, a slope of 1:3, a damage factor S of 2 and the normal 3000 waves in a storm that attacks the breakwater. This example breakwater assumed to be double layered.

Firstly, the ξ value is determined to be 1.84. Since $\xi_{transition}$ is 3.05, the plunging breaker type has to be used. The C_{pl} becomes then 7.71 and the armour porosity 35.5%, assuming a standard placement method and given that blockiness is 60,8% and elongation is 2.85 *m*.

With these values filled in the Van der Meer equation for plunging breakers a Dn50 is determined of 0.785 m. The required size of rock from this quarry is then estimated to be at least 0.80 m, the heap of rocks that was measured/ investigated would not be sufficiently stable in this example breakwater.

It can be concluded that a small exercise is carried out determining what the quality of the rock in a quarry is for hydraulic engineering purposes. The use of parameters as elongation and blockiness is tested. It is easy to see that the because of the enlargement of the C_{pl} and C_{su} due the fact that blockiness and elongation is known, smaller stone can be used.

The main problem in using these results in practice is the statistical reliability of all the data used. In the exercise done that reliability is far to small due to too small sample sizes. That yielded the large deviations from a log-Gaussian distribution for the D_{n50} unreliable blockiness and elongation parameters based on only 4 measurements and no clarity in the density of the rock since one sample can never be representative.

Also a quick look at the norms EN 13383 that specifies test methods for natural, artificial and recycled aggregates for use as armour stone, shows that the tests cannot be representative, since samples of 200 pieces are required for materials

in this weight class.

However neglecting these drawbacks it is made clear that investigations at the quarry site can be useful in reducing the stone-size needed. However, it should always be weighted whether the costs of these investigations are exceeded by the profits made with the smaller rocks used.

figure 9.5 Plot of d_n on a log gauss scale

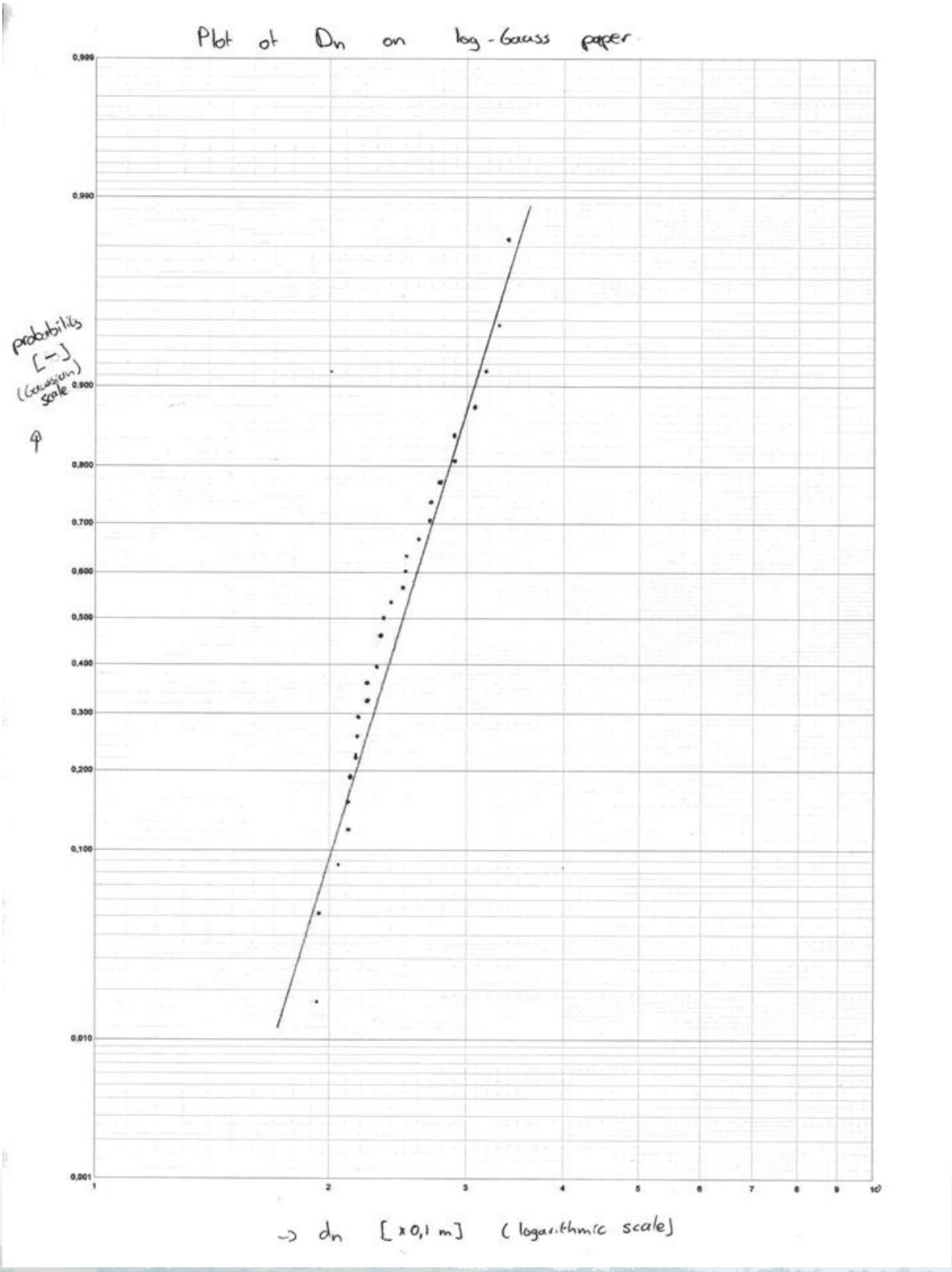

References

Introduction to Bed, bank and shore protection
G. J. Schiereck ISBN 90-407-1683-8

Breakwater and Closure dams
K. d'Angremond; F.C. van Roode ISBN 90-407-2127-0

Waves in Oceanic and Coastal Waters
L. H. Holthuijsen ISBN-13: 9780521860284

Introduction to Coastal Engineering and Management
J.W. Kamphuis ISBN 978-981-02-3830-8

Coastal engineering manual (CEM)
n/a ISBN 90 382 0412 4

Manual on the use of rock in coastal and shoreline engineering (SP083)
CIRIA ISBN 978-0-86017-326-7

Short Waves – reader
J. Battjes *et al.*

Empirical formula for breakage of Dolosse and Tetrapods
H.F. Burcharth, K. d'Angremond, J.W. van der Meer, Z. Liu Coastal Eng. 40_2000.183–206

CRESS – Coastal & River Engineering Support System
www.cress.nl

SURFER – Contouring, Gridding, and Surface Mapping
www.goldensoftware.com

Appendix I Beach Profiles

Measurements morning group north of the revetment

Comments on the measurements

The groups that measured the northern beach did not have the availability of a GPS receiver. Therefore the waterline was used as a reference for these measurements. The parallel distance was measured from the revetment to the point on the waterline along the beach. After that the measurements were taken perpendicular to the coastline to create the beach profiles. After the measurements, the points were coupled to the coordinates by measuring the angle with the UTM x-axis. Because the distance between the several points was known, it was possible to recalculate the coordinates of the measuring points. With this information it was possible to include this information in the surfer map.

table I.1 Profile A: distance from the revetment is 20 m, α=17°

Distance from cliff	0	1	2	3	4	5	6	6.5	8	11
Elevation of the slope	1.25	1.1	0.88	0.9	0.57	0.45	0.49	0.2	0	-0.1
Eastern coordinate	572143.5	572144.5	572145.5	572146.5	572147.5	572148.5	572149.5	572150	572151.5	572154.5
Northern coordinate	4743880	4743880	4743880	4743880	4743880	4743880	4743880	4743880	4743880	4743880
									BSL	clay

Remarks
α is the angle between the direction of the profile and the East

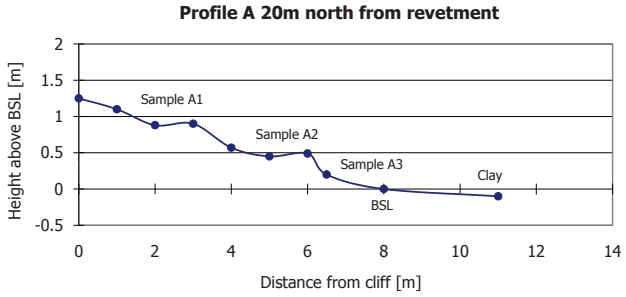

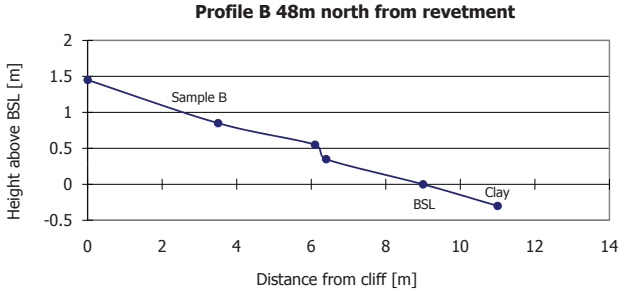

table I.2 Profile B: distance from the revetment is 48 m, α=21°

distance from cliff	0	3.5	6.1	6.4	9	11
measured value	*1*	*1.6*	*1.9*	*2.1*	*2.45*	*2.75*
elevation of the slope	1.45	0.85	0.55	0.35	0	-0.3
eastern coordinate	572148	572151.5	572154.1	572154.4	572157	572159
northern coordinate	4743902	4743902	4743902	4743902	4743902	4743902
					BSL	Clay

table I.3 Profile C: distance from the revetment is 70 m, α=16°

distance from cliff	0	3	5.3	5.5	8.7	11.6
measured value	*1*	*1.6*	*1.77*	*2.1*	*2.55*	*3.04*
elevation of the slope	1.55	0.95	0.78	0.45	0	-0.49
eastern coordinate	572152.8	572155.8	572158.1	572158.3	572161.5	572164.4
northern coordinate	4743923	4743923	4743923	4743923	4743923	4743923
					BSL	Clay

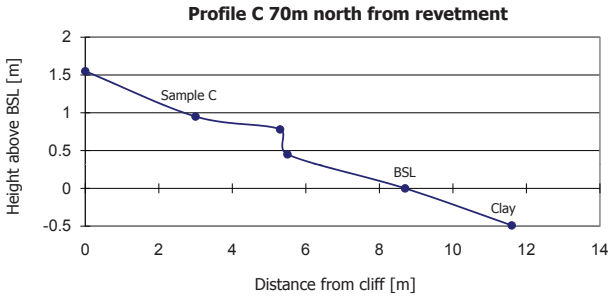

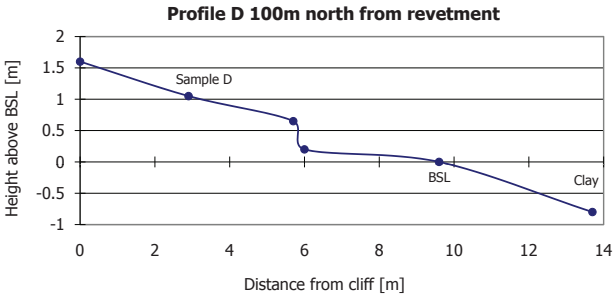

table I.4 Profile D: distance from the revetment is 100 m, α=0°

distance from cliff	0	2.9	5.7	6	9.6	13.7
measured value	*1*	*1.55*	*1.95*	*2.4*	*2.6*	*3.4*
elevation of the slope	1.6	1.05	0.65	0.2	0	-0.8
eastern coordinate	572155.9	572158.8	572161.6	572161.9	572165.5	572169.6
northern coordinate	4743953	4743953	4743953	4743953	4743953	4743953
					BSL	Clay

table I.5 Profile E: distance from the revetment is 130 m, α=0°

distance from cliff	0	2.6	4.8	7.3	9.3	13.5
measured value	*1*	*1.5*	*1.6*	*1.9*	*2*	*2.4*
elevation of the slope	1	0.5	0.4	0.1	0	-0.4
eastern coordinate	572160.2	572162.8	572165	572167.5	572169.5	572173.7
northern coordinate	4743983	4743983	4743983	4743983	4743983	4743983
					BSL	Clay

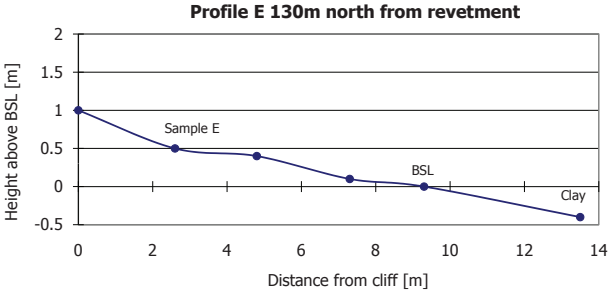

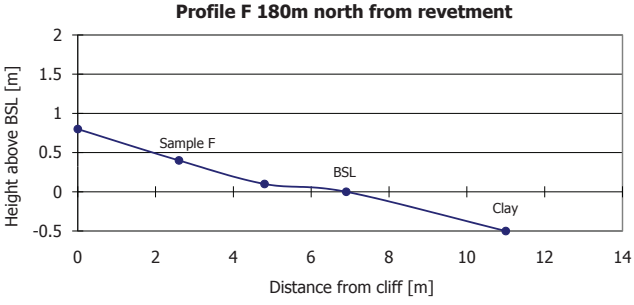

table I.6 Profile F: distance from the revetment is 180 m, α=25°

distance from cliff	0	2.6	4.8	6.9	11
measured value	*1*	*1.4*	*1.7*	*1.8*	*2.3*
elevation of the slope	0.8	0.4	0.1	0	-0.5
eastern coordinate	572175.1	572177.7	572179.9	572182	572186.1
northern coordinate	4744038	4744038	4744038	4744038	4744038
				BSL	Clay

table I.7 Profile G: distance from the revetment is 230 m, α=31°

distance from cliff	0	1.6	4.7	7.3	10.1	11
measured value	*1*	*1.5*	*1.9*	*2*	*2.05*	*2.2*
elevation of the slope	1.05	0.55	0.15	0.05	0	-0.15
eastern coordinate	572196.9	572198.5	572201.6	572204.2	572207	572207.9
northern coordinate	4744084	4744084	4744084	4744084	4744084	4744084
					BSL	Clay

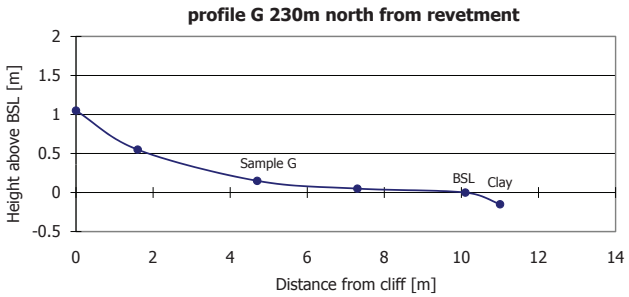

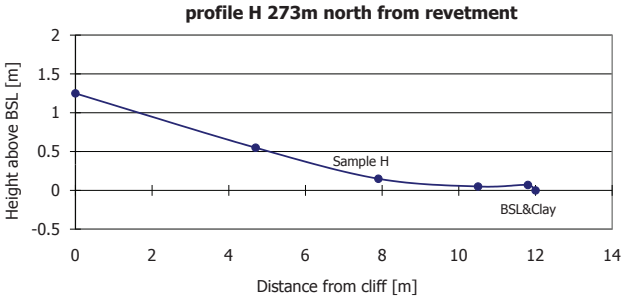

table I.8 Profile H: distance from the revetment is 273 m, α=23°

distance from cliff	0	4.7	7.9	10.5	11.8	12
measured value	*1*	*1.7*	*2.1*	*2.2*	*2.18*	*2.25*
elevation of the slope	1.25	0.55	0.15	0.05	0.07	0
eastern coordinate	572203	572207.7	572210.9	572213.5	572214.8	572215
northern coordinate	4744124	4744124	4744124	4744124	4744124	4744124
						BSL & clay

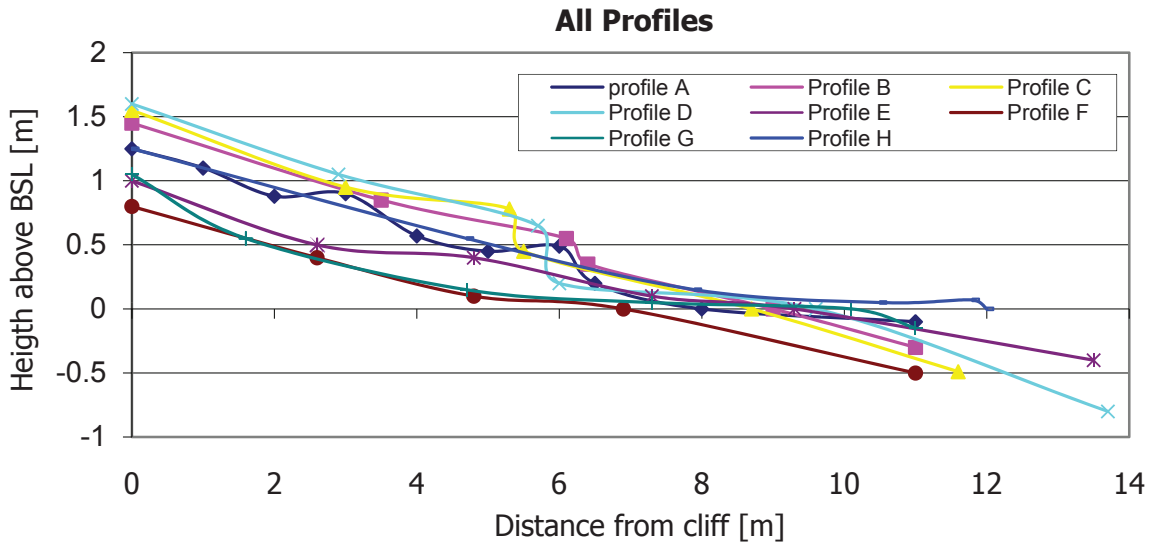

figure I.1 Overview all beach profiles north of revetment, measured by morning group

Measurements afternoon group north of the revetment

Comment on the measurements

During processing of the data it was noticed that the afternoon group made some mistakes and that they didn't measure several distances between the points especially the distance from the mean waterline. Only three profiles were correct for drawing the profiles. This group also didn't do any measurements in the water. Because of the inaccuracy of these measurements it was decided not to include these results in the surfer map.

table I.9 Profile I: 0 m north of revetment

Distance from cliff	**0**	**3.6**	**4**	**7.5**
Measured value	*0.95*	*1.75*	*1.95*	*2.4*
Elevation of the slope	1.45	0.65	0.45	0
				BSL

table I.10 Profile J: 132 m north of revetment

Distance from cliff	**0**	**3.5**	**7**	**11.2**
Measured value	*0.95*	*1.25*	*1.7*	*2.4*
Elevation of the slope	1.45	1.15	0.7	0
				BSL

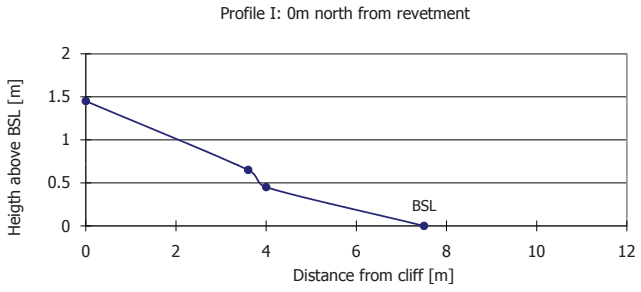

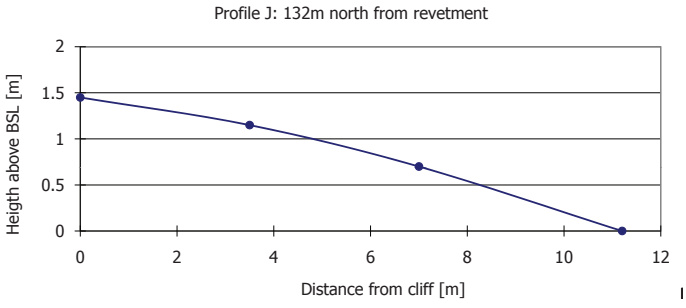

table I.11 Profile K: 90 m north of revetment

Distance form cliff	0	4	7.4	10
Measured value	0.95	1.6	1.85	2.5
Elevation of the slope	1.55	0.9	0.65	0
				BSL

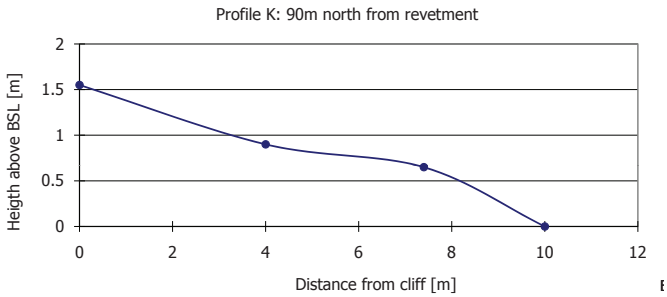

Measurements morning group south of the revetment

Comment on the measurements

Since the morning group used the baseline, GPS and the leveling instrument, the results they obtained were more accurate than those of the north beach. This group also made profiles of different length because the beach is wider.

The values on the x-axis of the graph are the distances from the baseline this group has set. The negative direction is the seaside. The positive direction is the landside.

table I.12 Profile L: 0 m south of revetment

Distance from baseline	3	2	1	0	-1	-2	-3	-4	-5	-6	-7	-8	-9
Elevation of the slope	1.11	1.11	1.22	1.14	0.97	0.68	0.55	0.45	0.24	0.23	0.04	-0.06	-0.24

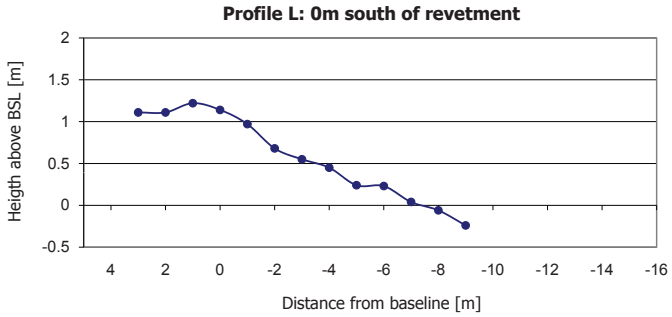

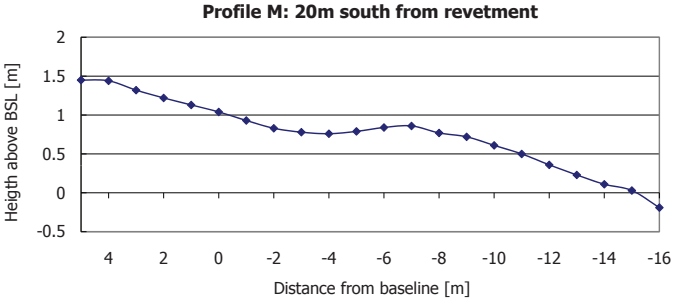

table I.13 Profile M: 20 m south of revetment

Distance from baseline	5	4	3	2	1	0	-1	-2	-3	-4	-5
Elevation of the slope	1.45	1.44	1.32	1.22	1.13	1.04	0.93	0.83	0.78	0.76	0.79

Distance from baseline	-6	-7	-8	-9	-10	-11	-12	-13	-14	-15	-16
Elevation of the slope	0.84	0.86	0.77	0.72	0.61	0.5	0.36	0.23	0.11	0.03	-0.19

table I.14 Profile N: 60 m south of revetment

Distance from baseline	16	15	14	13	12	11	10	9	8	7	6	5	4	3
Elevation of the slope	1.99	1.92	1.88	1.78	1.62	1.48	1.37	1.23	1.14	1.02	0.93	0.83	0.72	0.71

Distance from baseline	2	1	0	-1	-2	-3	-4	-5	-6	-7	-8	-9	-10	-11
Elevation of the slope	0.71	0.74	0.79	0.75	0.64	0.54	0.53	0.55	0.55	0.29	0.12	-0.03	-0.2	-0.35

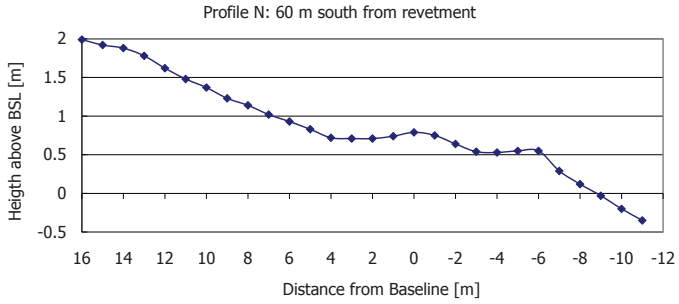

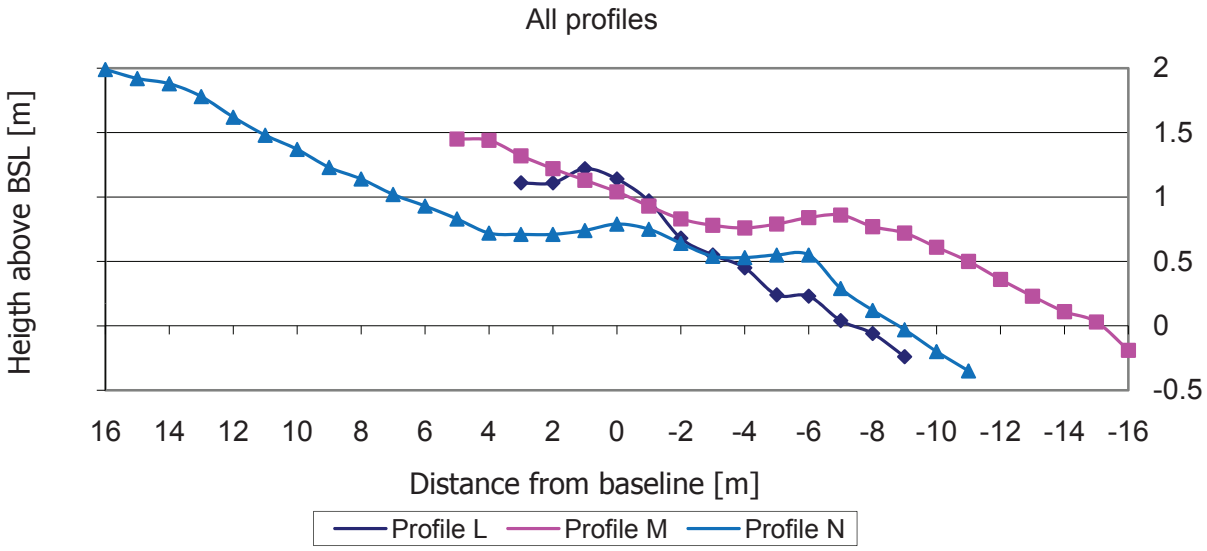

figure I.2 Overview beach profiles south of revetment, measured by morning group

Measurements afternoon group south of the revetment

Comment on the measurements

The afternoon group used the same method. The only difference is that this group measured a shorter distance from the waterline. Also for only the first profile a student was willing to enter the water. The other profiles are measured until the end of the wave run-up.

table I.15 Profile O: 89 m south of revetment

Distance from baseline	16	3	-2	-4	-9.5	-10.75	-13	-16.3	-19.5
Elevation of the slope	2.22	0.77	0.86	0.84	0	-0.08	-0.45	-0.56	-0.5

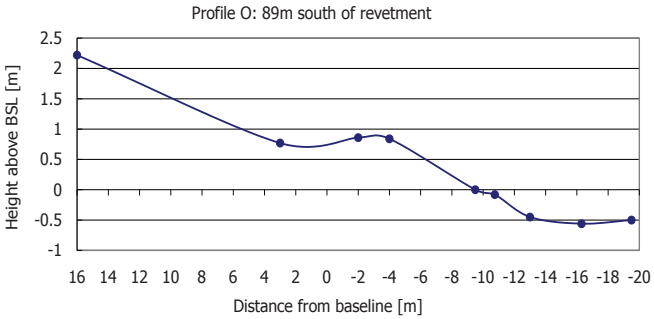

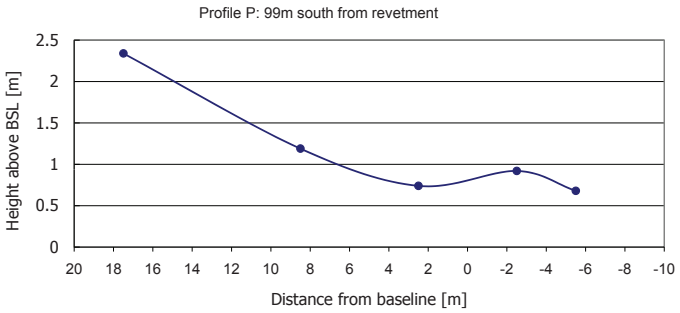

table I.16 Profile P: 99 m south of revetment

Distance from baseline	17.5	8.5	2.5	-2.5	-5.5
Elevation of the slope	2.34	1.19	0.74	0.92	0.68

table I.17 Profile Q: 109 m south of revetment

Distance from baseline	21	10	4	-3	-5.5
Elevation of the slope	1.99	0.8	0.91	0.91	0.72

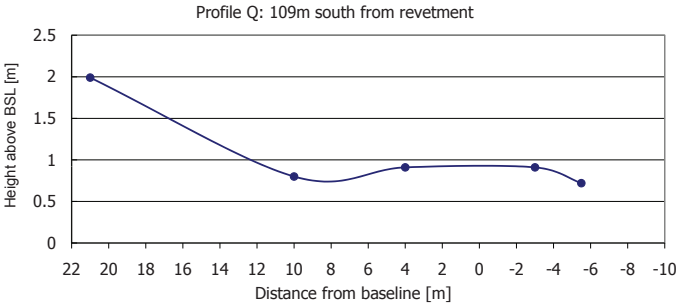

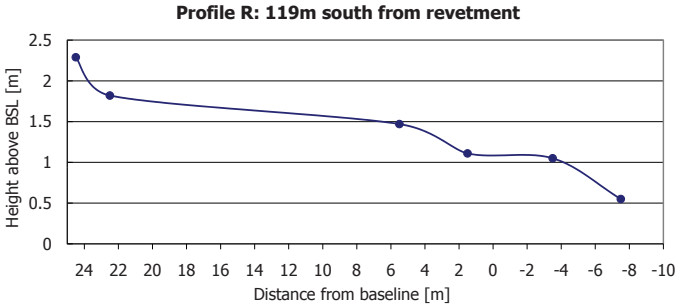

table I.18 Profile R: 119 m south of revetment

Distance from baseline	24.5	22.5	5.5	1.5	-3.5	-7.5
Elevation of the slope	2.29	1.82	1.47	1.11	1.05	0.55

table I.19 Profile S: 129 m south of revetment

Distance from baseline	29	27	9	4	-4	-7
Elevation of the slope	2.29	1.79	1.35	1.19	1.04	0.73

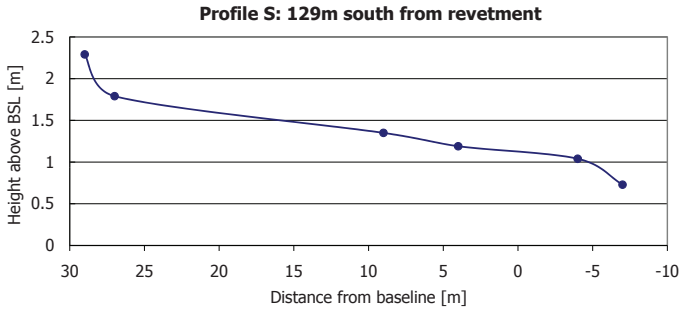

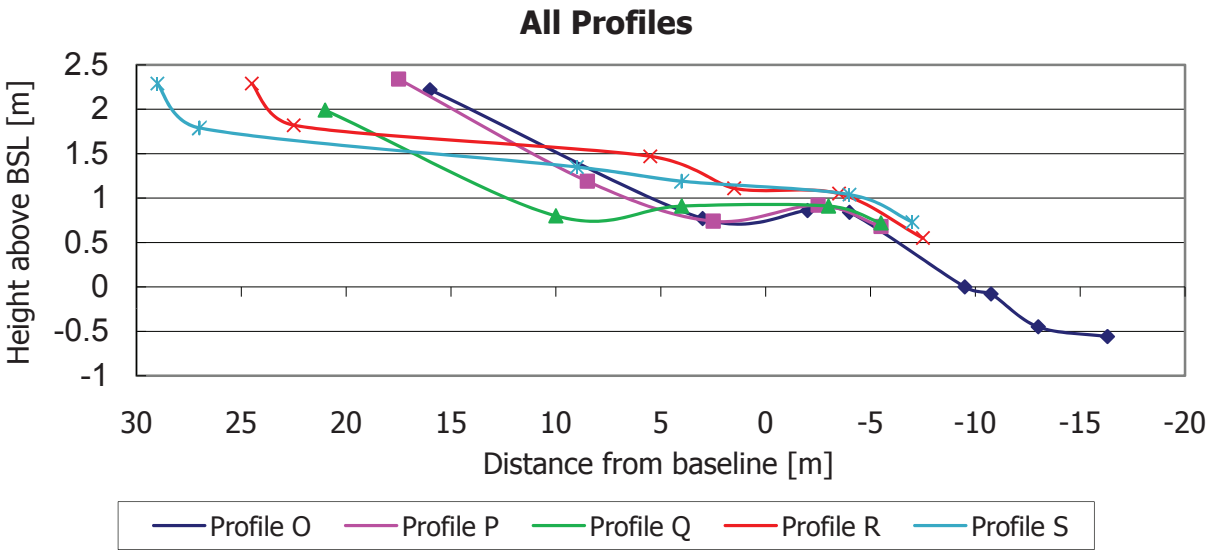

figure I.3 Overview beach profiles south of revetment, measured by afternoon group

table V.1 Overview sieve analyses

Sample 1			Description	SOUTH OF REVETMENT, BEACH PROFILE SOUTH													
	D50	0,53	Date	10/7/2006													
	D60 / D10	1,87	Sieve diameter [mm]	1,400	1,180	0,850	0,710	0,600	0,500	0,425	0,355	0,250	0,212	0,180	0,150	0,125	< 0,125
			Weight [g]	2,325	2,104	12,804	13,678	24,941	32,321	24,824	20,062	19,901	2,815	1,262	0,586	0,170	

Sample 2			Description	SOUTH OF REVETMENT, BEACH PROFILE NORTH													
	D50	0,45	Date	10/7/2006													
	D60 / D10	2,00	Sieve diameter [mm]	1,400	1,180	0,850	0,710	0,600	0,500	0,425	0,355	0,250	0,212	0,180	0,150	0,125	< 0,125
			Weight [g]	3,237	2,666	18,217	18,513	19,575	17,198	16,614	23,513	53,176	11,099	4,170	1,760		

Sample 3a			Description	NORTH OF REVETMENT, BEACH PROFILE A1 (above waterlevel, near cliff)													
	D50	0,50	Date	10/7/2006													
	D60 / D10	1,56	Sieve diameter [mm]	1,400	1,180	0,850	0,710	0,600	0,500	0,425	0,355	0,250	0,212	0,180	0,150	0,125	< 0,125
			Weight [g]	0,000	0,000	2,345	7,720	28,345	47,625	32,588	28,424	21,920	0,438	1,011			

Sample 3b			Description	NORTH OF REVETMENT, BEACH PROFILE A2 (above waterlevel, on berm)													
	D50	0,91	Date	10/7/2006													
	D60 / D10	1,47	Sieve diameter [mm]	1,400	1,180	0,850	0,710	0,600	0,500	0,425	0,355	0,250	0,212	0,180	0,150	0,125	< 0,125
			Weight [g]	7,151	17,713	91,910	30,850	17,470	6,230	0,830	0,220	0,100	0,030				

Sample 3c			Description	NORTH OF REVETMENT, BEACH PROFILE A3 (at waterline)													
	D50	0,57	Date	10/7/2006													
	D60 / D10	1,56	Sieve diameter [mm]	1,400	1,180	0,850	0,710	0,600	0,500	0,425	0,355	0,250	0,212	0,180	0,150	0,125	< 0,125
			Weight [g]	0,000	0,570	10,658	18,894	46,030	53,249	19,494	13,362	11,384	0,741	0,342			

Sample 4			Description	NORTH OF REVETMENT, BEACH PROFILE B1													
	D50	0,40	Date	10/7/2006													
	D60 / D10	1,39	Sieve diameter [mm]	1,400	1,180	0,850	0,710	0,600	0,500	0,425	0,355	0,250	0,212	0,180	0,150	0,125	< 0,125
			Weight [g]	0,000	0,035	0,731	1,130	4,539	17,726	37,951	52,440	37,791	1,781	0,476	0,186	0,360	

table V.1 Overview sieve analyses (continued)

Sample 5			Description	NORTH OF REVETMENT, BEACH PROFILE C1													
	D50	0,62	Date	10/7/2006													
	D60 / D10	1,66	Sieve diameter [mm]	1,400	1,180	0,850	0,710	0,600	0,500	0,425	0,355	0,250	0,212	0,180	0,150	0,125	< 0,125
			Weight [g]	4,883	4,865	33,142	27,067	41,105	43,093	25,569	16,718	9,072	0,253	0,091			

Sample 6			Description	NORTH OF REVETMENT, BEACH PROFILE D1													
	D50	0,52	Date	10/7/2006													
	D60 / D10	1,42	Sieve diameter [mm]	1,400	1,180	0,850	0,710	0,600	0,500	0,425	0,355	0,250	0,212	0,180	0,150	0,125	< 0,125
			Weight [g]	0,000	1,613	14,247	16,821	34,869	71,960	59,820	38,021	17,078	0,421	0,074	0,083		

Sample 7			Description	NORTH OF REVETMENT, BEACH PROFILE E1													
	D50	0,50	Date	10/7/2006													
	D60 / D10	1,54	Sieve diameter [mm]	1,400	1,180	0,850	0,710	0,600	0,500	0,425	0,355	0,250	0,212	0,180	0,150	0,125	< 0,125
			Weight [g]	0	0,844	9,033	14,434	25,290	39,332	38,304	30,999	15,757	0,708	0,230	0,187		

Sample 8			Description	NORTH OF REVETMENT, BEACH PROFILE F1													
	D50	0,55	Date	10/7/2006													
	D60 / D10	1,49	Sieve diameter [mm]	1,400	1,180	0,850	0,710	0,600	0,500	0,425	0,355	0,250	0,212	0,180	0,150	0,125	< 0,125
			Weight [g]	0,000	0,958	10,775	14,713	42,224	70,890	30,404	19,437	9,590	0,177	0,162			

Sample 9			Description	NORTH OF REVETMENT, BEACH PROFILE G1													
	D50	0,63	Date	10/7/2006													
	D60 / D10	1,84	Sieve diameter [mm]	1,400	1,180	0,850	0,710	0,600	0,500	0,425	0,355	0,250	0,212	0,180	0,150	0,125	< 0,125
			Weight [g]	0,000	3,294	34,771	27,500	30,779	30,151	16,580	14,119	13,963	0.900	0,282	0,376		

Sample 10			Description	NORTH OF REVETMENT, BEACH PROFILE H1													
	D50	0,41	Date	10/7/2006													
	D60 / D10	1,52	Sieve diameter [mm]	1,400	1,180	0,850	0,710	0,600	0,500	0,425	0,355	0,250	0,212	0,180	0,150	0,125	< 0,125
			Weight [g]	0,000	0,223	1,225	1,933	7,630	28,809	38,386	43,665	45,850	3,540	1,198	0,471	0,382	

Sample 11a			Description	TIP OF BREAKWATER, SHOAL INSIDE HARBOUR													
	D50	0,28	Date	10/9/2006													
	D60 / D10	1,50	Sieve diameter [mm]	1,400	1,180	0,850	0,710	0,600	0,500	0,425	0,355	0,250	0,212	0,180	0,150	0,125	< 0,125
			Weight [g]	0,000	0,000	0,265	0,351	1,089	3,342	6,644	15,477	71,980	29,770	14,670	5,500	0,960	0,37

Sample 11b			Description	TIP OF BREAKWATER, BETWEEN TETRAPODS ON TOP													
	D50	0,39	Date	10/9/2006													
	D60 / D10	2,00	Sieve diameter [mm]	1,400	1,180	0,850	0,710	0,600	0,500	0,425	0,355	0,250	0,212	0,180	0,150	0,125	< 0,125
			Weight [g]	2,800	2,220	12,040	9,324	14,419	21,030	18,015	24,013	50,813	13,956	6,026	3,401	1,175	1,577

Sample 12			Description	BASE OF BREAKWATER, BEACH NORTH													
	D50	0,65	Date	10/9/2006													
	D60 / D10	1,69	Sieve diameter [mm]	1,400	1,180	0,850	0,710	0,600	0,500	0,425	0,355	0,250	0,212	0,180	0,150	0,125	< 0,125
			Weight [g]	2,229	3,732	30,279	26,302	32,162	26,666	15,192	10,428	6,778	0,407	0,140			

Sample 13a			Description	BIALA BEACH, ABOVE WATERLEVEL													
	D50	0,40	Date	10/9/2006													
	D60 / D10	1,65	Sieve diameter [mm]	1,400	1,180	0,850	0,710	0,600	0,500	0,425	0,355	0,250	0,212	0,180	0,150	0,125	< 0,125
			Weight [g]	0,000	0,270	2,267	2,607	7,983	21,810	33,502	44,291	48,644	3,291	0,805	0,320		

Sample 13b			Description	BIALA BEACH, ON WATERLINE													
	D50	0,58	Date	10/9/2006													
	D60 / D10	1,71	Sieve diameter [mm]	1,400	1,180	0,850	0,710	0,600	0,500	0,425	0,355	0,250	0,212	0,180	0,150	0,125	< 0,125
			Weight [g]	0,678	2,971	29,248	19,988	30,401	34,082	24,726	20,348	12,538	0,397	0,212			

Sample 14a			Description	SKOR BEACH, ABOVE WATERLEVEL													
	D50	0,74	Date	10/9/2006													
	D60 / D10	1,91	Sieve diameter [mm]	1,400	1,180	0,850	0,710	0,600	0,500	0,425	0,355	0,250	0,212	0,180	0,150	0,125	< 0,125
			Weight [g]	6,768	12,062	59,614	35,493	37,636	27,402	14,308	10,877	9,318	0,884				

Sample 14b			Description	SKOR BEACH, ON WATERLINE													
	D50	0,53	Date	10/9/2006													
	D60 / D10	1,61	Sieve diameter [mm]	1,400	1,180	0,850	0,710	0,600	0,500	0,425	0,355	0,250	0,212	0,180	0,150	0,125	< 0,125
			Weight [g]	3,819	3,664	16,074	12,462	20,545	32,180	28,333	21,972	13,040	0,355	0,155			

table V.2 Sieve sampe 1

Sample 1			Description	SOUTH OF REVETMENT, BEACH PROFILE SOUTH												
	D50	0,53	Date	10/7/2006												
	D60 / D10	1,87	Sieve diameter [mm]	1,400	1,180	0,850	0,710	0,600	0,500	0,425	0,355	0,250	0,212	0,180	0,150	0,125	< 0,125
			Weight [g]	2,325	2,104	12,804	13,678	24,941	32,321	24,824	20,062	19,901	2,815	1,262	0,586	0,170	
	cumulative			2,325	4,429	17,233	30,911	55,852	88,173	112,997	133,059	152,96	155,775	157,037	157,623	157,793	
	%			1,473	2,807	10,921	19,590	35,396	55,879	71,611	84,325	96,937	98,721	99,521	99,892	100	
	% passing sieve			98,527	97,193	89,079	80,410	64,604	44,121	28,389	15,675	3,063	1,279	0,479	0,108	0	
	P (passing sieve)			0,985	0,972	0,891	0,804	0,646	0,441	0,284	0,157	0,031	0,013	0,005	0,001	0	
	inverse distribution			2,177	1,910	1,231	0,856	0,375	-0,148	-0,571	-1,008	-1,872	-2,233	-2,591	-3,068		

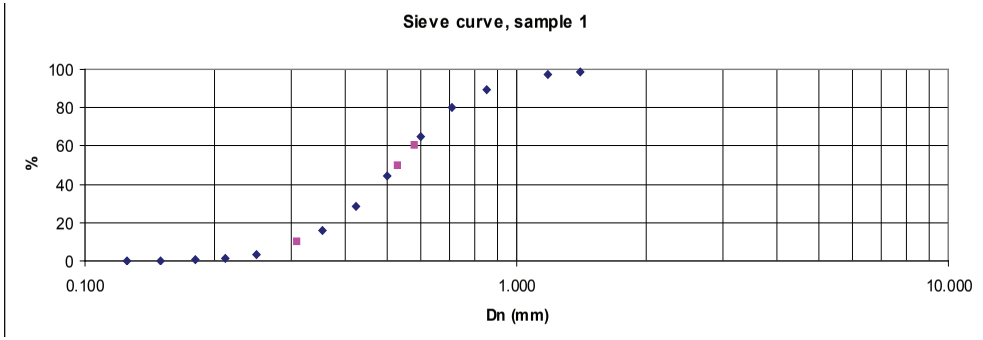

figure V.1 Sieve Curve; sample 1

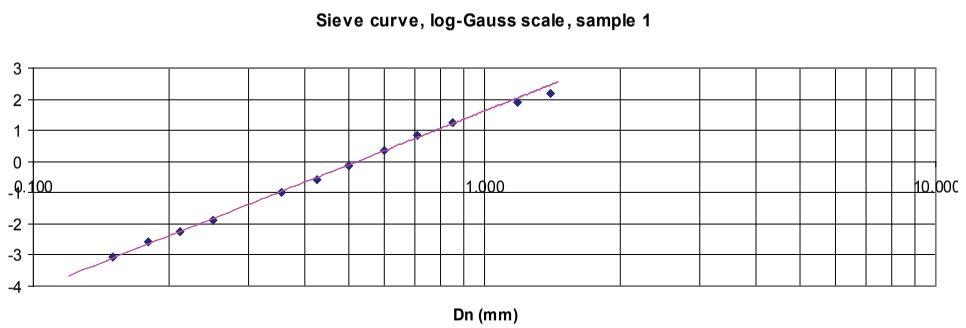

figure V.2 Sieve Curve on log Gauss scalel; sample 1

table V.3 Sieve sampe 2

Sample 2			Description	SOUTH OF REVETMENT, BEACH PROFILE NORTH												
	D50	0,45	Date	10/7/2006												
	D60 / D10	2,00	Sieve diameter [mm]	1,400	1,180	0,850	0,710	0,600	0,500	0,425	0,355	0,250	0,212	0,180	0,150	0,125	< 0,125
			Weight [g]	3,237	2,666	18,217	18,513	19,575	17,198	16,614	23,513	53,176	11,099	4,170	1,760		
	cumulative			3,237	5,903	24,120	42,633	62,208	79,406	96,020	119,533	172,709	183,808	187,978	189,738		
	%			1,706	3,111	12,712	22,469	32,786	41,850	50,607	62,999	91,025	96,875	99,072	100		
	% passing sieve			98,294	96,889	87,288	77,531	67,214	58,150	49,393	37,001	8,975	3,125	0,928	0		
	P (passing sieve)			0,983	0,969	0,873	0,775	0,672	0,581	0,494	0,370	0,090	0,031	0,009	0		
	inverse distribution			2,119	1,865	1,140	0,756	0,446	0,206	-0,015	-0,332	-1,342	-1,863	-2,354			

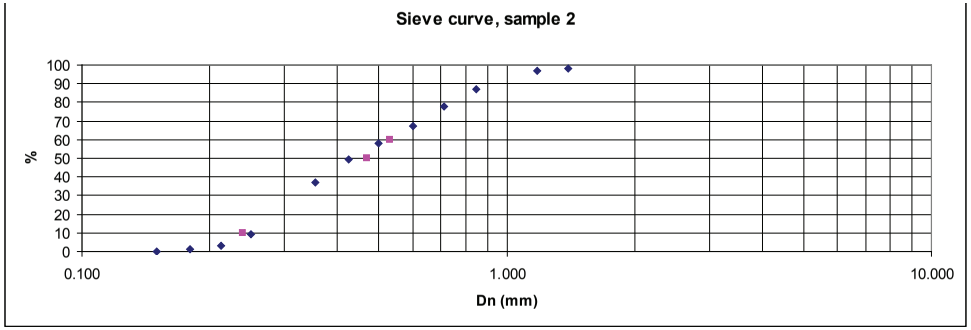

figure V.3 Sieve Curve; sample 2

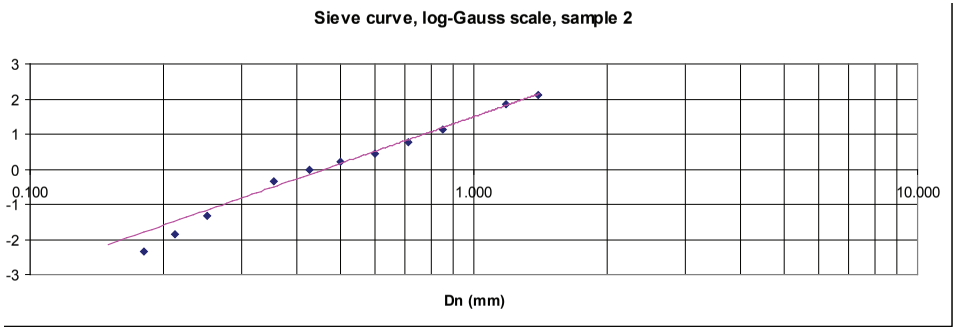

figure V.4 Sieve Curve on log Gauss scalel; sample 2

table V.3 Sieve sampe 3a

Sample 3a			Description	NORTH OF REVETMENT, BEACH PROFILE A1 (above waterlevel, near cliff)													
	D50	0,50	Date	10/7/2006													
	D60 / D10	1,56	Sieve diameter [mm]	1,400	1,180	0,850	0,710	0,600	0,500	0,425	0,355	0,250	0,212	0,180	0,150	0,125	< 0,125
			Weight [g]	0,000	0,000	2,345	7,720	28,345	47,625	32,588	28,424	21,920	0,438	1,011			
	cumulative			0,000	0,000	2,345	10,065	38,410	86,035	118,623	147,047	168,967	169,405	170,416			
	%			0,000	0,000	1,376	5,906	22,539	50,485	69,608	86,287	99,150	99,407	100,000			
	% passing sieve			100,000	100,000	98,624	94,094	77,461	49,515	30,392	13,713	0,850	0,593	0,000			
	P (passing sieve)			1,000	1,000	0,986	0,941	0,775	0,495	0,304	0,137	0,009	0,006	0,000			
	inverse distribution					2,204	1,563	0,754	-0,012	-0,513	-1,093	-2,387	-2,516				

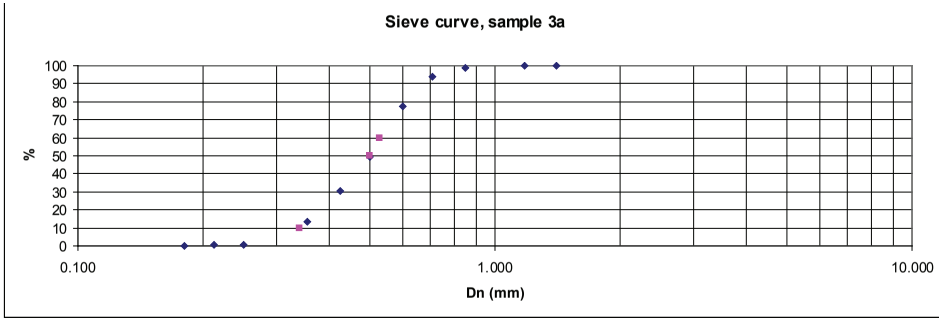

figure V.5 Sieve Curve; sample 3a

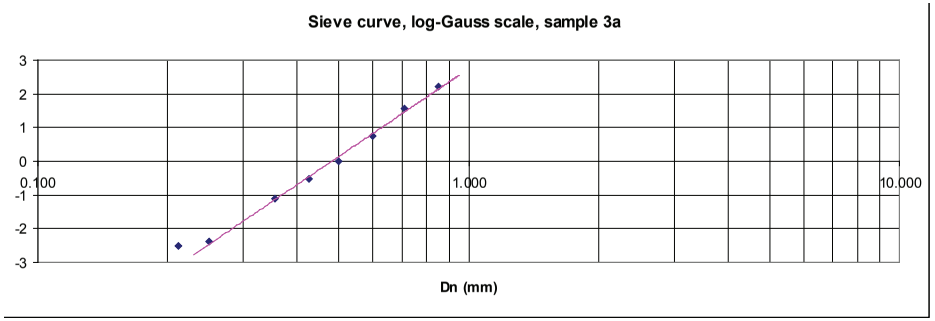

figure V.6 Sieve Curve on log Gauss scalel; sample 3a

Please note:
The rest of the sieve samples where done in the same extended way. They are not included in these appendixes.

Appendix VI The Visser approximation

In the equation to determine the surface elevation, one of the parameters is the wave number. The wave number is determined by

$$k = \frac{2\pi}{L}$$

Where L is the transitional water depth wave length.

The transitional water depth wave length is determined by

$$L = \frac{gT^2}{2\pi} \tanh kh$$

In this equation a wave number is required, which is one of the parameters we have to determine. Via this way the wave number is very difficult to determine. To resolve this problem, dr.ir. P.J. Visser made an approximation for the transitional water depth wave length:

$$L = \sqrt{gh} \bullet \left(1 - \frac{h}{L_0}\right) T \quad for \quad \frac{h}{L_0} < 0.36$$

$$L = L_0 \qquad for \quad \frac{h}{L_0} \geq 0.36$$

With

$$L_0 = \frac{gT^2}{2\pi} \approx 1.56T^2$$

With this approximation the wave number k can be determined.

Appendix VII Formulae for determination significant wave height

$$\bar{f}_h = \sqrt{\frac{m_2}{m_0}} \exp(-\frac{h^2}{2m_0}) \qquad \bar{f}_0 = \sqrt{\frac{m_2}{m_0}}$$

Interpreting this relative number as the probability of $\bar{\eta}_{crest}$ exceeding the level η gives:

$$\Pr\{\bar{\eta}_{crest} > \eta\} = \frac{\bar{f}_\eta}{\bar{f}_0} = \frac{\sqrt{\frac{m_2}{m_0}} \exp(-\frac{\eta^2}{2m_0})}{\sqrt{\frac{m_2}{m_0}}} = \exp(-\frac{\eta^2}{2m_0})$$

So that the cumulative distribution function $\Pr\{\bar{\eta}_{crest} < \eta\} = 1 - \Pr\{\bar{\eta}_{crest} > \eta\}$ is:

$$P_{\bar{\eta}_{crest}}(\eta) = 1 - \exp(-\frac{\eta^2}{2m_0})$$

$$H_s = 4\sqrt{m_0}$$

Then $P_{\bar{\eta}_{crest}}(\eta) = 1 - \exp(-\frac{\eta^2}{2m_0})$ can be rewritten as $P_{\bar{\eta}_{crest}}(H) = 1 - \exp(-(\frac{2H}{H_s})^2)$

The probability density function of H is obtained as the derivative of $P_{H_{crest}}(H)$:

$$p_{H_{crest}}(H) = \frac{4H}{H_s} \exp(-(\frac{2H}{H_s})^2)$$

These functions are of the Rayleigh type.

A Rayleigh distribution has only one parameter, which in this case happens to be the significant wave height .

And the significant wave height = $H_s = \frac{1}{N/3}\sum_{j=1}^{N/3} H_j$

Where j is not the sequence number in the record but the rank number of the wave, based on wave height.

The significant wave height and significant wave period determined by the 492 records are H_s= 0,85 *m*, T_s = 5.64 *s*

In the following graph, we plot the distribution of the observed wave heights against the Rayleigh distribution, in which blue line stands for the Rayleigh distribution and the red star line stands for the real distribution. From the graph we can see there is some similarity between the real distribution and the Rayleigh distribution. The overestimation of the waves is due to the low accuracy of the equipment.

figure VI.1I Reyleigh distribution of the wave height

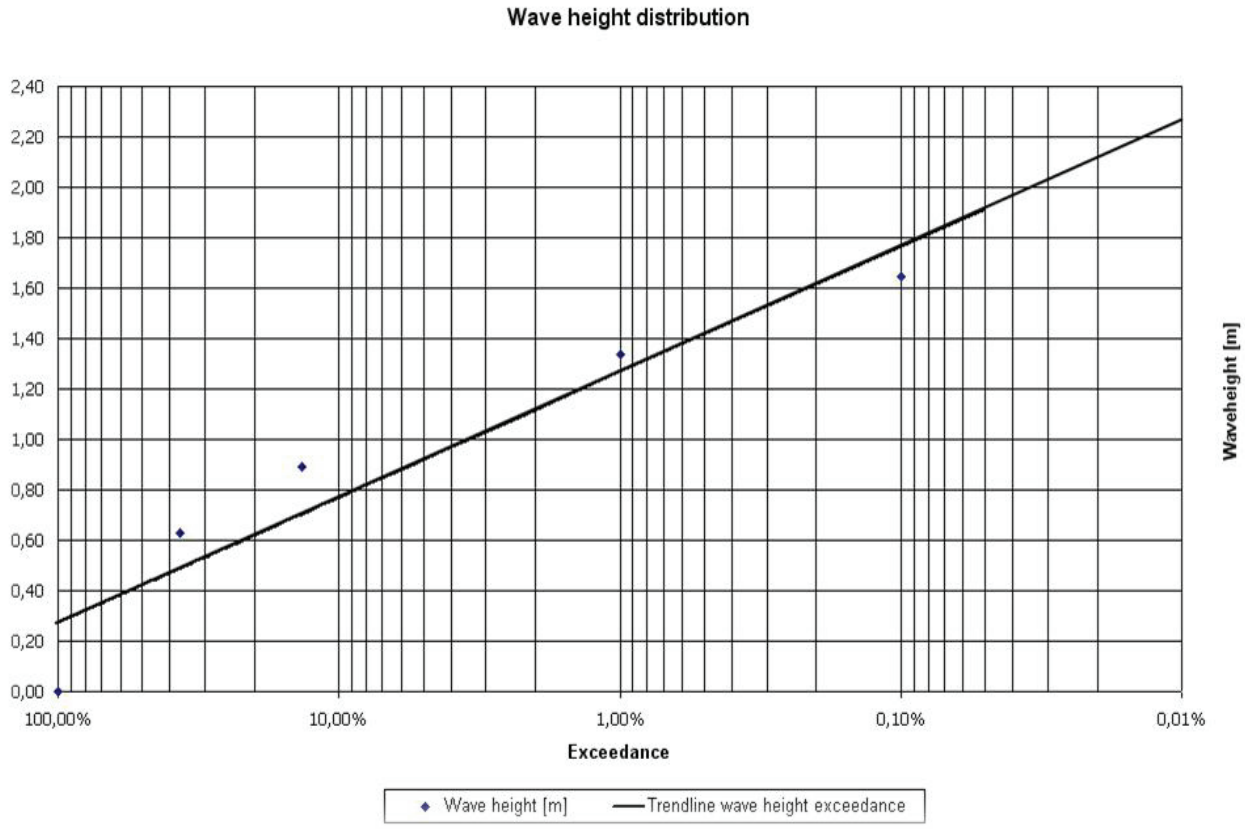

Appendix IX Results from CRESS

table IX.1 CRESS data

		Return period once per year			Return period once per 10 year			Return period once per 100 year		
distance from shore	**Waterdepth**	**H_s summer**	**H_s middle**	**H_s winter**	**H_s summer**	**H_s middle**	**H_s winter**	**H_s summer**	**H_s middle**	**H_s winter**
1600	-9,3	2,53	3,3	5,49	3	4,04	7,08	3,56	4,65	8,72
1400	-9	2,46	3,09	4,17	2,84	3,57	4,63	3,2	3,84	5,02
1200	-8,5	2,39	2,93	3,76	2,71	3,31	4,09	3	3,51	4,36
1000	-8	2,31	2,79	3,48	2,59	3,11	3,75	2,84	3,27	3,98
800	-7,2	2,22	2,64	3,24	2,47	2,92	3,47	2,68	3,06	3,68
700	-6,7	2,17	2,56	3,11	2,39	2,81	3,33	2,58	2,94	3,52
600	-6,3	2,11	2,46	2,96	2,31	2,69	3,17	2,48	2,81	3,35
500	-6	2,05	2,36	2,81	2,23	2,57	3,01	2,38	2,68	3,18
400	-5,5	1,98	2,26	2,68	2,14	2,45	2,86	2,28	2,55	3,02
300	-5	1,89	2,14	2,51	2,03	2,31	2,68	2,16	2,4	2,84
200	-4,5	1,79	2	2,33	1,91	2,15	2,49	2,02	2,23	2,65
155	-4	1,73	1,93	2,25	1,84	2,07	2,41	1,94	2,14	2,56
110	-3,5	1,63	1,81	2,11	1,73	1,94	2,27	1,83	2,01	2,42
65	-3	1,5	1,65	1,92	1,59	1,77	2,08	1,67	1,83	2,24
45	-2,5	1,42	1,56	1,83	1,5	1,67	1,99	1,58	1,74	2,15
35	-2	1,35	1,49	1,76	1,43	1,6	1,93	1,51	1,67	2,1
25	-1,5	1,2	1,33	1,61	1,28	1,44	1,79	1,35	1,51	1,98
15	-1	0,97	1,08	1,37	1,03	1,19	1,57	1,1	1,26	1,78
5	-0,5	0,66	0,76	1,06	0,71	0,86	1,29	0,77	0,93	0,93
0	0	0	0	0	0	0	0	0	0	0

Notation

Distance from shore in meters
Waterdepth in meters
H_s = Significant wave height in meters

Appendix VIII Presentation Byala

As held on October 11th, 2006

Purpose of the fieldwork
Цели на учебната практика

- At university students learn theory
  В Университета студентите получават главно теоретични познания:

Университет по архитектура,строителство и геодезия
София,България
Faculty of Civil Engineering and Geosciences
Section Hydraulic Engineering
Delft, The Netherlands

TU Delft

- At university students learn how to make a design:
  В Университета студентите се научават и да проектират:
  - Given a, b, c => calculate X, Y, Z
    => design something
  - При зададени a, b, c => изчисляват X, Y, Z
    => проектират нещо

  - During fieldwork students learn to determine a, b, c
    По време на практиката студентите се научават да определят a, b, c

Additional objective
(Допълнителни цели)

- How to translate the questions of client into technical boundary conditions

  Как да приведат въпросите на клиента към техническата страна на граничните условия

Университет по архитектура,строителство и геодезия
София,България
Faculty of Civil Engineering and Geosciences
Section Hydraulic Engineering
Delft, The Netherlands
TU Delft

Introduction
Въведение

- To design a breakwater boundary conditions are needed
  Нужда от определяне на граничните условия

- Objective: Determine boundary conditions
  - Bathymetry
  - Waves
  - Morphology

  Цели: Определяне на граничните условия
  - Батиметрия
  - Вълнови режим
  - Морфология

Interaction of boundary conditions
Взаимодействие между граничните условия

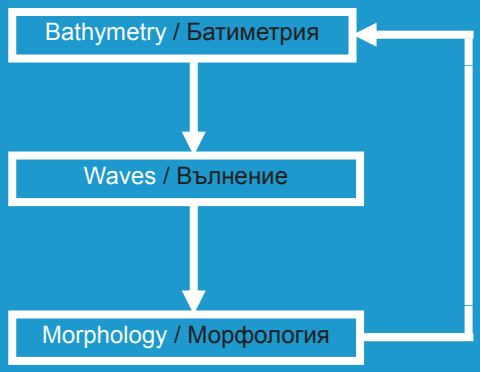

Университет по архитектура,строителство и геодезия
София,България
Faculty of Civil Engineering and Geosciences
Section Hydraulic Engineering
Delft, The Netherlands
TU Delft

Bathymetry
Батиметрия

Why is information needed?
Защо ни е необходима тази информация?

- Determination of the wave height
  Определяне на височината на вълните
- Needed for breakwater design
  Проектиране на вълнолома

Университет по архитектура,строителство и геодезия
София,България
Faculty of Civil Engineering and Geosciences
Section Hydraulic Engineering
Delft, The Netherlands

TU Delft

Bathymetry (2)
Батиметрия (2)

What is measured?
Какво е измерено?

Университет по архитектура,строителство и геодезия
София,България
Faculty of Civil Engineering and Geosciences
Section Hydraulic Engineering
Delft, The Netherlands

TU Delft

Bathymetry (3)
Батиметрия (3)

Results

Резултати

Университет по архитектура,строителство и геодезия
София,България
Faculty of Civil Engineering and Geosciences
Section Hydraulic Engineering
Delft, The Netherlands

TU Delft

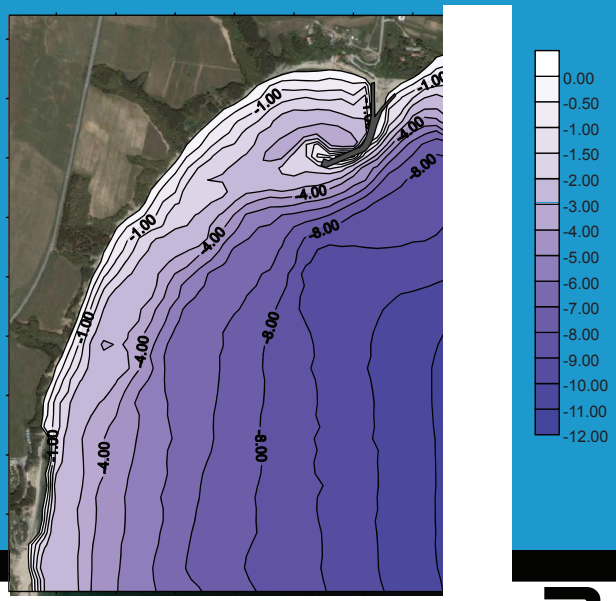

TU Delft
Delft University of Technology

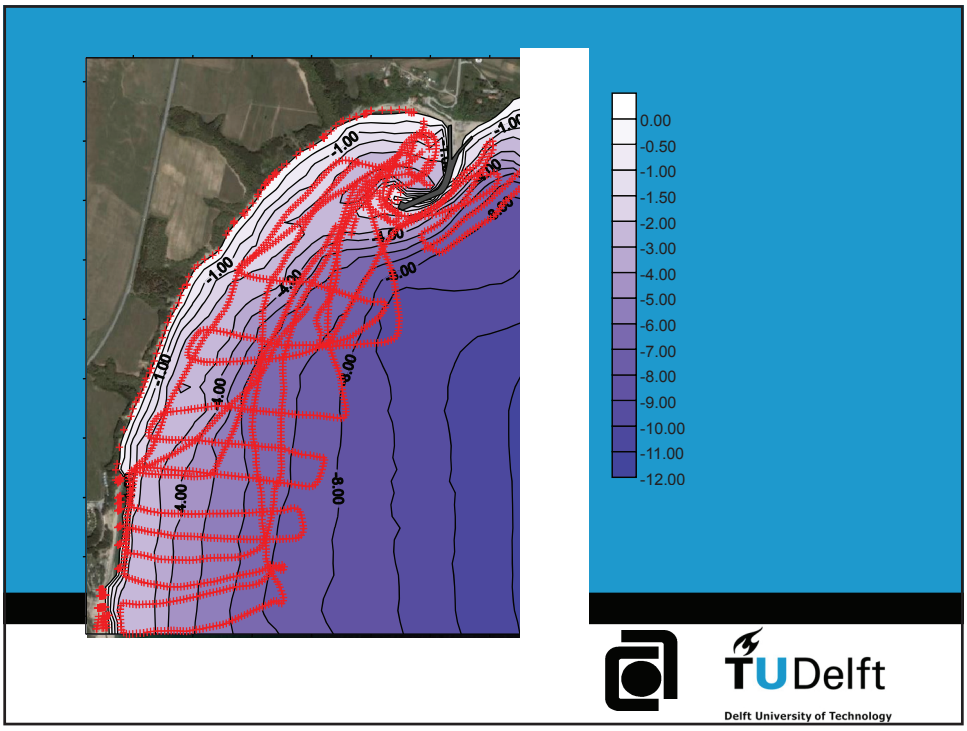

Wave heights
Височина на вълните

Why needed?

Защо е необходимо?

- Needed for breakwater design

  За проектиране на вълнолома

  - Crest height

    Кота било вълнолом

  - Rock size

    Размер на защитните блокове

- Waves influence sediment transport

  Въздействие на вълнението върху транспорта на наноси

Wave heights (2)
Височина на вълните (2)

What did we measure?
Какво е измервано?

Wave heights (3)
Височина на вълните (3)

•Deep water wave statistics are used
•Вероятностни характеристики на вълнението в дълбоководието

•Checked it with measurements
•Проверка чрез измервания

•Patterns
•План на вълнението

Wave heights (4)
Височина на вълните (4)

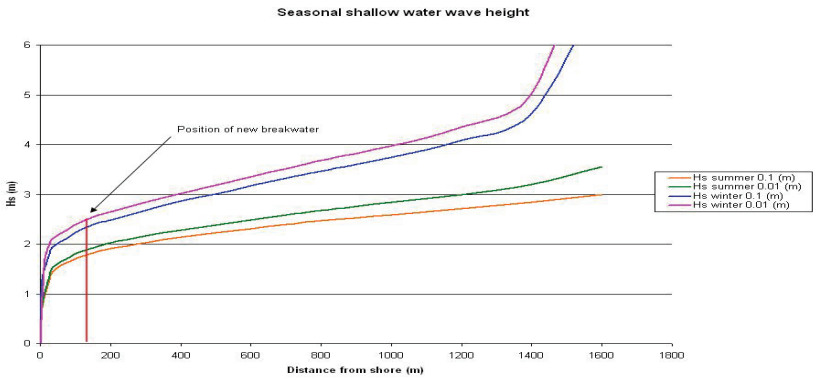

Университет по архитектура,строителство и геодезия
София,България
Faculty of Civil Engineering and Geosciences
Section Hydraulic Engineering
Delft, The Netherlands
TU Delft

Morphology
Морфология

What is morphology?
Какво е морфология?

- Transport of sediments
  Транспорт на наноси
- Depositions of sediment
  Отлагане
- Erosion
  Ерозия

Morphology (2)
Морфология (2)

Why needed?
Защо е необходимо?

- Deposition in marina is not good
  Отлагането на наноси в пристанището - нежелателно
- Erosion or sedimentation?
  Ерозия или отлагания?

Morphology (3)
Морфология (3)

What did we measure?
Какво е измервано?

•Samples to get insight into actual transport processes of sediment
Проби за добиване на представа за характера на наносните процеси

•Visual observations
Наблюдения

Design requirements for the breakwater
Начални изисквания за вълнолома

- Marina only in use in summer

Ползване на пристанището само през летния сезон

- In winter take boats out

Извеждане на плавателните съдове през зимата

- No quay wall on the breakwater

Без кей зад вълнолома

  - Advantage: overtopping is allowed

  Предимства: Допустимо преливане

- Design height based on probability

  Оразмерителна височина базирана на вероятностни характеристики

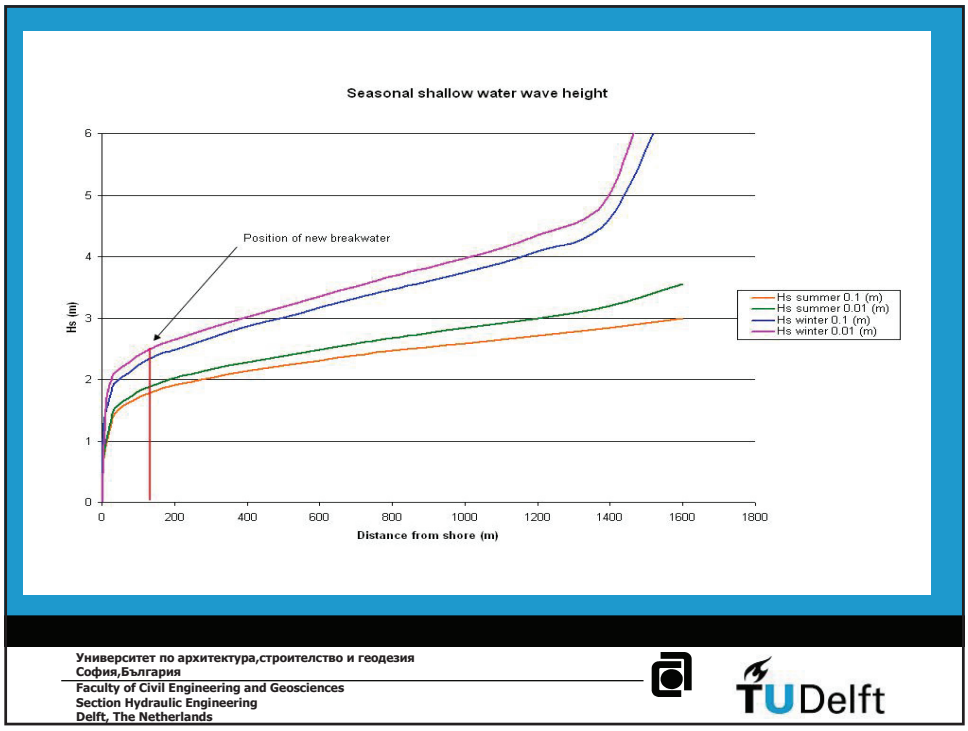

Университет по архитектура,строителство и геодезия
София,България
Faculty of Civil Engineering and Geosciences
Section Hydraulic Engineering
Delft, The Netherlands

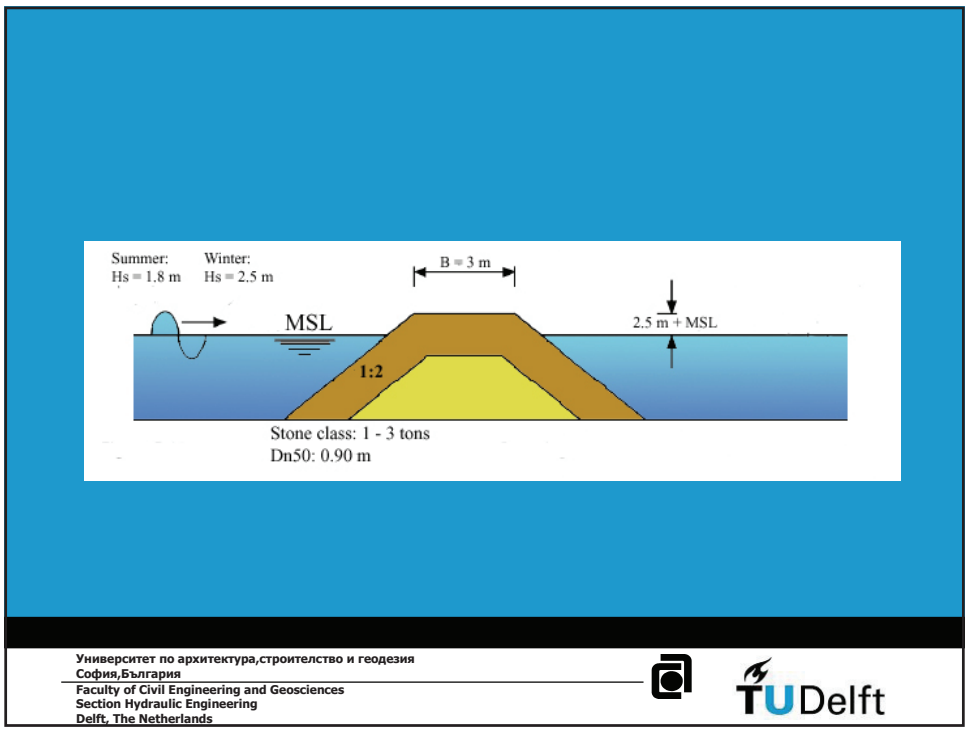

Университет по архитектура,строителство и геодезия
София,България
Faculty of Civil Engineering and Geosciences
Section Hydraulic Engineering
Delft, The Netherlands

Conclusions
Заключения

- Preliminary boundary conditions are determined
  Определени са началните гранични условия

- Important differences between existing and future breakwater
  Съществени различия между съществуващия и бъдещия вълнолом
  - Functioning
    Функционалност
  - Location
    Разположение

Университет по архитектура,строителство и геодезия
София,България
Faculty of Civil Engineering and Geosciences
Section Hydraulic Engineering
Delft, The Netherlands

Appendix X Tetrapod breakwater design wave calculation

Hudson

$$M = \frac{\rho_s H_{sc}^{\ 3}}{K_D \Delta^3 \cot\alpha} \quad (\text{or: } \frac{H_{sc}}{\Delta d} = \sqrt[3]{K_D \cot\alpha})$$

Type 1

_=	1,23	
d=	1,094348	m
K_D=	5	
_=	45	degrees
cot(_)=	1	
H_{sc}=	2,30171	m

Type 2

_=	1,23	
d=	1,426057	m
K_D=	5	
_=	45	degrees
cot(_)=	1	
H_{sc}=	2,999384	m

Van der Meer

tan(α)=	0,50	$\xi_m = \frac{\tan(\alpha)}{\sqrt{s_m}}$		tan(α)=	1
s_m=	0,05			s_m=	0,05
ξ=	2,24			ξ=	4,47

Plunging waves (ξ<3)

$$\frac{H_s}{\Delta D_n} = \left(8.6\left(\frac{N_{od}}{\sqrt{N}}\right)^{0.5} + 3.94\right) s_m^{0.2}$$

Type 1

D_n=	1,09	m	
Δ=	1,23		
N_{od}=	0,2	(damage level 0.2 to 0.5)	
N=	7500	(number of waves)	
s_m=	0,05		
H_s=	3,22	m	

Type 2

D_n=	1,43	m	
Δ=	1,23		
N_{od}=	0,2	(damage level 0.2 to 0.5)	
N=	7500	(number of waves)	
s_m=	0,05		
H_s=	4,19	m	

Surging waves (ξ>3)

$$\frac{H_s}{\Delta D_n} = \left(3.75\left(\frac{N_{od}}{\sqrt{N}}\right)^{0.5} + 0.85\right) s_m^{-0.2}$$

Type 1

D_n=	1,09	m	
Δ=	1,23		
N_{od}=	0,2	(damage level 0.2 to 0.5)	
N=	7500	(number of waves)	
s_m=	0,05		
H_s=	2,52	m	

Type 2

D_n=	1,43	m	
Δ=	1,23		
N_{od}=	0,2	(damage level 0.2 to 0.5)	
N=	7500	(number of waves)	
s_m=	0,05		
H_s=	3,29	m	

Hanzawa

$$= \frac{H_s}{\Delta D_n} = 2.32 \left(N_{od} / N_z^{0.5} \right)^{0.2} + 1.33$$

Type 1

D_n=	1,09	m
€=	1,23	
N_{od}=	0,2	
N_z=	7500	
H_s=	2,72	m

Type 2

D_n=	1,43	m
€=	1,23	
N_{od}=	0,5	
N_z=	7500	
H_s=	3,78	m

Appendix XI Breakage of the Tetrapods

The breakage of the Tetrapods can be determined by equation XI.1 [Burcharth (2000)]

$$B = C_0 M^{C_1} S^{C_2} H_s^{C_3}$$ equation XI.1

B = relative breakage
M = armour unit mass in tons
S = concrete tensile strength in *MPa*
H_s = significant wave height in *m*
η = water elevation in *m*
C_0, C_1, C_2, C_3 = fitted parameters

Chosen are the following parameters, based on Burcharth (2000)

C_0 = 0.00393
C_1 = -0.79
C_2 = -2.73
C_3 = 3.84
$C_{0,variational}$ = 0.25

Based on measurements

M_{type1} = 3.0 *ton*
M_{type2} = 6.6 *ton*
H_s = 2.5 *m*

Determined following from visual observation

S = 2 *MPa*

When the parameters are applied into equation XI.1 the results are as follows:

For type 1 elements

B(5 % upper limit) = 1.19 percent

B(5% lower limit) = 0.49 percent

For type 2 elements

B(5 % upper limit) = 0.64 percent

B(5% lower limit) = 0.26 percent

Appendix XII Rubble mound breakwater stone size determination

$$N_s^* = N_s \left(H_s / L_p\right)^{-1/3} = \frac{H_s}{\Delta D_{n50}} \left(H_s / L_p\right)^{-1/3}$$

equation XII.1

H_s = 2.5 *m* (Winter)
$\rho(s)$ = 2400 *kg/m³*
$\rho(w)$ = 1000 *kg/m³*
Δ = 1.4
N_s = 2 (mobility parameter, see table XII.1)
D_{n50} = 0.89
W_{50} = 1708 *kg*
Stone class = 1 -3 tons

table XII.1 Mobility parameter

Regime	$N_s = Ho$	$HoTo$
Little movement; non-reshaping	< 1.5 – 2	< 20 – 40
Limited movement during reshaping; statically stable	1.5 – 2.7	40 – 70
Relevant movement, reshaping; dynamically stable	> 2.7	> 70

Note:

*) The criteria depend to some extent on the rock gradation

Appendix XIII Rubble mound breakwater crest height determination

Wave overtopping

$$R^* = R_c \Big/ \left(T_m \left(g H_s \right)^{0.5} \right)$$

$$Q^* = a \exp\left(-b R^* / \mathrm{g} \right)$$

$$Q^* = q \Big/ \left(T_m g H_s \right)$$

equation XIII.1

H_s = 1.8 *m* (Summer)
T_m = 5.94 *m*
s_m = 0.03
ξ_m = 2.77
a = 0.01
b = 21.60
R_c = 2.00 *m*
γ = 0.55

R^* = 0.08
Q^* = 0.00
q = 42.34 *l/s*

Wave transmission

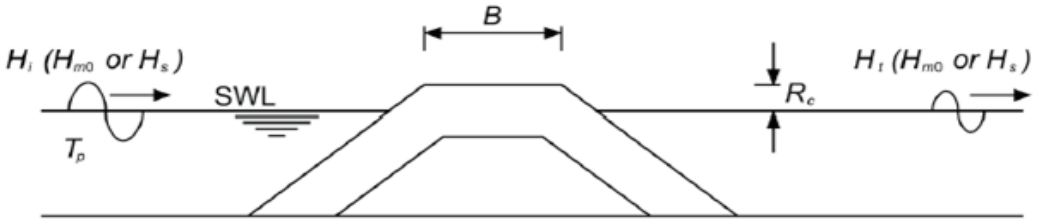

$$C_t = -0.4 R_c / H_s + 0.64 \left(B / H_s \right)^{-0.31} \left(1 - e^{-0.5 \mathrm{x}_p} \right) \qquad C_t = H_t / H_i = \sqrt{E_t / E_i}$$

equation XIII.2

R_c = 2.00 *m*
H_s = 1.8 *m* (Summer)
B = 3 *m*
tan(α) = 0.5
ξ_m = 2.77
T_p = 6.6 *s*
ξ_p = 0

C_t = 0.63686
H_t = 0 *m*

Appendix XIV Probabilistic analysis of rubble mound breakwater

Rubble mound breakwater in 3 m of water

PIANC Partial Coefficients		
PF	GAM(er)	GAM s
0,5	1,06	1,03
0,156	1,29	1,07
0,1	1,38	1,08
0,05	1,51	1,11
0,01	1,79	1,17
0,001	2,27	1,25

	Rock	Tetra	Tetra 2	
rho water	1010	1010	1010	
Kd	4	5	5	Breaking waves
slope breakwater	1,5	1,5	1,5	
rho stone	2650	2300	2600	
delta	1,6237624	1,277227723	1,574257426	
Km	0,2132182	0,189399784	0,224098211	

ds	3,0	Depth at structure [m]
db	4,0	Breaker depth [m]
m	0,02	Slope at structure [-]

(Sigma) s =Sigma H	0,15	
Sigma slope	0,1	
Sigma mass	0,25	
Sigma Kd	0,15	
Sigma delta	0,05	
Sigma rho water	0,05	
(Sigma) r	0,23	

Breaker wave height	Hsb	2,4
Conventional Hsb:	Hsbmax=	1,80
Case A: Mod. depth lim.wWave:	Hsbmax'=	1,95
Case B: mod. Cum. depth lim.	Hmax=	2,92

CASE A - Level I - Hdes & Pe = 1 (regular occuring waves)

				Stone	Tetra 1	Tetra 2	DeltaM tetra (%)
Case A.1.1	Deterministic	Hdes=	1,95	Km= 0,213	0,189	0,224	
				M= 760	1085	655	-40%
Case A.1.2	(PIANC - Pf=0.5)						
		Hdes=	1,95	Km= 0,213	0,189	0,224	
		Gam(er)=	1,06	M= 990	1412	852	-40%
		Gam(s)=	1,03				
		Mur=	2,12				
Case A.1.3	(PIANC - Pf=0.1)						
		Hdes=	1,95	Km= 0,213	0,189	0,224	
		Gam(er)=	1,38	M= 2517	3591	2168	-40%
		Gam(s)=	1,08				
		Mur=	2,90				

CASE A - Level II - Hdes & Pe = 1 (regular occuring waves)

	(Mu)s	(Sigma')s	(Sigma')r	Gams*Gamr	Gamz	Gamma	(Mu)r	Beta
Case A.2.1	1,95	0,15	0,23	1,1	1,05	1,155	2,25	0,503
Case A.2.2	1,95	0,15	0,23	1,38	1,08	1,490	2,90	1,295
Case A.2.3	1,95	0,17	0,23	1,38	1,08	1,490	2,90	1,267

Calculated Values

Pf	PL	M stone	M Tetra1	M Tetra2
0,308	0,308	1172	1671	1009
0,098	0,098	2517	3591	2168
0,103	0,103	2517	3591	2168

CASE B - Level I - Hdes,cum & Pe = 1 (regular occuring waves)

				Stone	Tetra 1	Tetra 2	DeltaM tetra (%)
Case B.1.1	Deterministic	Hdes=	2,92	Km= 0,213	0,189	0,224	
				M= 2566	3661	2210	-40%
Case B.1.2	(PIANC - Pf=0.5)						
		Hdes=	2,92	Km= 0,213	0,189	0,224	
		Gam(er)=	1,06	M= 3340	4765	2877	-40%
		Gam(s)=	1,03				
		Mur=	3,19				
Case B.1.3	(PIANC - Pf=0.1)						
		Hdes=	2,92	Km= 0,213	0,189	0,224	
		Gam(er)=	1,38	M= 8496	12121	7318	-40%
		Gam(s)=	1,08				
		Mur=	4,35				

CASE B - Level II - Hdes,cum & Pe = 1 (regular occuring waves)

	(Mu)s	(Sigma')s	(Sigma')r	Gams*Gamr	Gamz	Gamma'	(Mu)r	Beta
Case B.2.1	2,92	0,15	0,23	1,1	1,05	1,155	3,37	0,503
Case B.2.2	2,92	0,15	0,23	1,38	1,08	1,490	4,35	1,295
Case B.2.3	2,92	0,17	0,23	1,38	1,08	1,490	4,35	1,267

Calculated Values

Pf	PL	M Stone	M Tetra1	M Tetra2
0,308	0,308	3954	5641	3406
0,098	0,098	8496	12121	7318
0,103	0,103	8496	12121	7318

Appendix XV Quarry operation

The quarry which is discussed here is exploited by Bulgarian company. This company consists of four quarries, two of these produce cement; the others produce blocks for (rail-) road foundations, paint and glass production as well as an additive in food for animals. The latter is the quarry that is investigated.

This quarry has the maximum depth of 20 meters, according to Bulgarian safety regulations. The actual height of the quarry is varied between 18 and 21 meters. The limestone, approximately 95% is CaCO3, is sorted into different sizes. A first distinction can be made between rocks, pebbles, dust and fine dust.

Those large rocks are crushed firstly by jaw crushers as the primary separation. Afterward, they will be crushed by ball crushers in pebbles as the secondary sorting. The rocks that can not be handled by the jaw crushers are used for slope stability or hydraulic structures. The dust, the result of the separation, is obtained in various sizes; 5-30 mm, 25-60 mm and 60-150mm. Finally, they all are sorted and then sold to the customer correspondingly.

Technically, the dust (0-1 mm) calcium is extracted. This is used as an additive for animal food production in which the calcium has a size of 200-300 µm. The smaller parts that are left over, <200 µm will be crushed by the ball crusher and sorted into three different categories; 20-40 µm, 40-60 µm and 60-80 µm respectively.

In addition, before the separation of the dust take place, they are heated in an oven which temperature is of between 110-115 oC. Afterward, 1 1/2 tons of dust is collected per hour. The primary micro separation is a statical one. This is conducted in a sort of cone where a pneumatic pressure sorts out the dust of 60-80 µm. Due to their heaviest size and weight they will logically fall down into the first sorting bin, see figure XV.1 below. Afterward, a secondary separation is taken place dynamically. These components consist of fine filters and sieves. When they are full with dust it will be emptied into a bin.

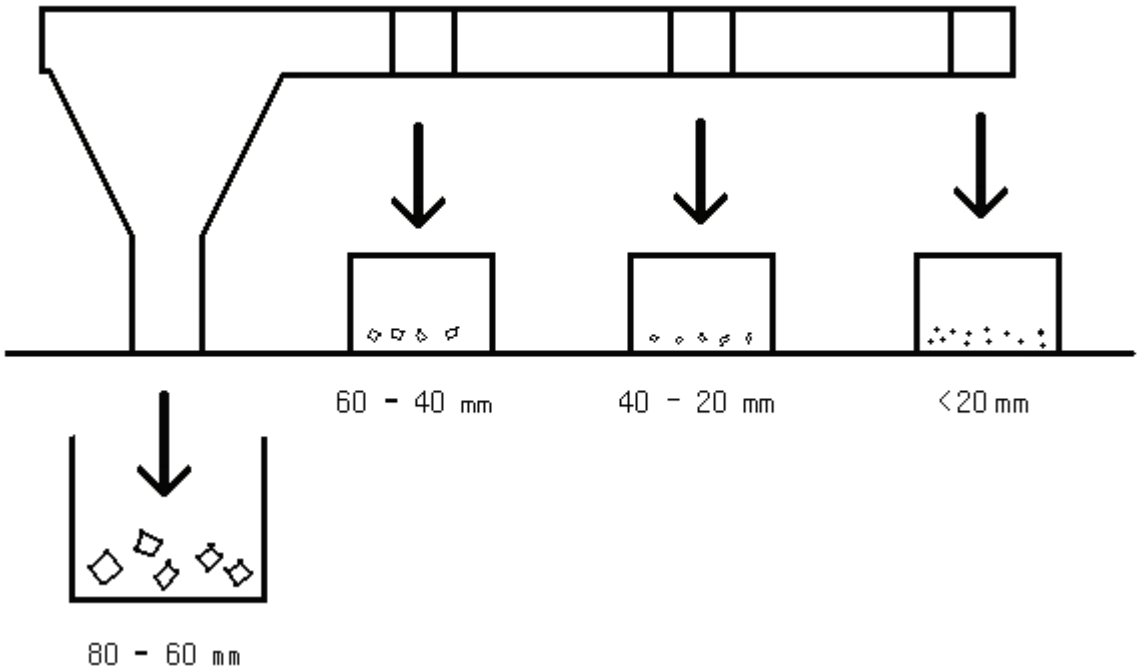

figure XV.1 Schematic of the sorting process

In conclusion, the production of the quarry can be expressed in term of logistic as per day about 60 – 80 trucks are arriving and leaving the quarry consequently. In addition, the quarry can sell almost 100% of its output from the sorting operation.

Appendix XVI Measurements quarry

table XVI.1 Measurements made at Martsiana quarry

		Elongation		Volume		
Number	**Weight** (*kg*)	**Longest** (*m*)	**Shortest** (*m*)	**Length** (*m*)	**Width** (*m*)	**Height** (*m*)
1	48,7	*0,50*	*0,13*	*0,34*	*0,51*	*0,20*
2	45,0					
3	56,5					
4	67,9					
5	26,5	*0,45*	*0,16*	*0,37*	*0,34*	*0,17*
6	40,5					
7	35,0					
8	36,5					
9	56,9	*0,52*	*0,20*	*0,50*	*0,30*	*0,30*
10	28,8					
11	16,5					
12	26,0					
13	23,7					
14	73,4	*0,45*	*0,21*	*0,39*	*0,38*	*0,29*
15	82,4					
16	23,3					
17	23,6					
18	36,1					
19	31,5					
20	22,3					
21	21,5					
22	21,7					
23	16,8					
24	25,9					
25	45,5					
26	29,9					
27	28,0					
28	20,4					
29	89,9					